AGU PUBLICATIONS

JGR

Journal of Geophysical Research: Oceans

RESEARCH ARTICLE

10.1002/2015JC011021

Do the Amazon and Orinoco freshwater plumes really matter for hurricane-induced ocean surface cooling?

O. Hernandez[1], J. Jouanno[1], and F. Durand[1]

[1]LEGOS, Université de Toulouse, CNES, CNRS, IRD, UPS

Key Points:
- Amplitude of TC-induced cooling is significantly reduced in Amazon and Orinoco plume regions
- Cooling difference between plume and open ocean waters are almost not sensitive to river runoff
- Thermal stratification is at leading order the main factor controlling the amplitude of cooling

Correspondence to:
O. Hernandez,
olgahernand@gmail.com

Citation:
Hernandez, O., J. Jouanno, and F. Durand (2016), Do the Amazon and Orinoco freshwater plumes really matter for hurricane-induced ocean surface cooling?, *J. Geophys. Res. Oceans*, *121*, 2119–2141, doi:10.1002/2015JC011021.

Received 4 JUN 2015
Accepted 5 MAR 2016
Accepted article online 11 MAR 2016
Published online 1 APR 2016

ABSTRACT Recent studies suggested that the plume of low-saline waters formed by the discharge of the Amazon and Orinoco rivers could favor Atlantic Tropical Cyclone (TC) intensification by weakening the cool wake and its impact on the hurricane growth potential. The main objective of this study is to quantify the effects of the Amazon-Orinoco river discharges in modulating the amplitude of TC-induced cooling in the western Tropical Atlantic. Our approach is based on the analysis of TC cool wake statistics obtained from an ocean regional numerical simulation with $^1/_4^\circ$ horizontal resolution over the 1998–2012 period, forced with realistic TC winds. In both model and observations, the amplitude of TC-induced cooling in plume waters (0.3–0.4°C) is reduced significantly by around 50–60% compared to the cooling in open ocean waters out of the plume (0.6–0.7°C). A twin simulation without river runoff shows that TC-induced cooling over the plume region (defined from the reference experiment) is almost unchanged (∼0.03°C) despite strong differences in salinity stratification and the absence of barrier layers. This argues for a weaker than thought cooling inhibition effect of salinity stratification and barrier layers in this region. Indeed, results suggest that haline stratification and barrier layers caused by the river runoff may explain only ∼10% of the cooling difference between plume waters and open ocean waters. Instead, the analysis of the background oceanic conditions suggests that the regional distribution of the thermal stratification is the main factor controlling the amplitude of cooling in the plume region.

1. Introduction

The western Tropical Atlantic Ocean is characterized by a body of warm waters forming the second largest warm pool of the word ocean [e.g., *Wang and Enfield*, 2001]. This region receives important amounts of continental freshwaters, with main contributions from the Amazon (210,000 m^3 of water per s) and Orinoco rivers (35,000 m^3 of water per s). As they flow into the ocean, they are spread off the coast to the north by the Guiana Current and eddies produced by the retroflexion of the North Brazil Current, or to the east by the North Equatorial Current. They influence the large scale salinity distribution in the region (Figure 1) and contribute to form barrier layers that can exceed 30 m thick [*Pailler et al*., 1999, *Mignot et al*., 2007].

As illustrated in Figure 1, tropical cyclones (TC) often pass directly over the plume. *Ffield* [2007] has shown that 68% of all category 5 Atlantic hurricanes during the 1960–2000 time period passed directly over the historical region of the plume, suggesting that the majority of the most destructive hurricanes may be influenced by ocean–atmosphere interaction within the plume just prior to reaching the Caribbean, and that the freshwater inputs from the Amazon and Orinoco could be active players of TC intensification in the region.

Two causal relationships between the river plumes and tropical cyclogenesis are generally proposed. First, the presence of particularly warm SSTs over river plumes could favor their development. This would be in agreement with modeling results by *Vizy and Cook* [2010] that show a great sensitivity of summertime climate and hurricane intensity and frequency to temperature anomalies over the Amazon-Orinoco plume region. Second, the inhibition of TC-induced surface cooling by the presence of strong haline stratification and barrier layers could favor TC intensification by weakening the cool wake and its impact on the hurricane growth potential [*Schade and Emanuel*, 1999; *Balaguru et al*., 2012a].

Indeed, the main response observed in the wake of TCs is the cooling of the surface waters. It can reach up to 10° C [*Chiang et al*., 2011], but the average cooling under TCs in a radius of 200 km around the track is generally of the order of 1°C [*Vincent et al*., 2012a, 2012b; *Neetu et al*., 2012, *Vincent et al*., 2014]. The main

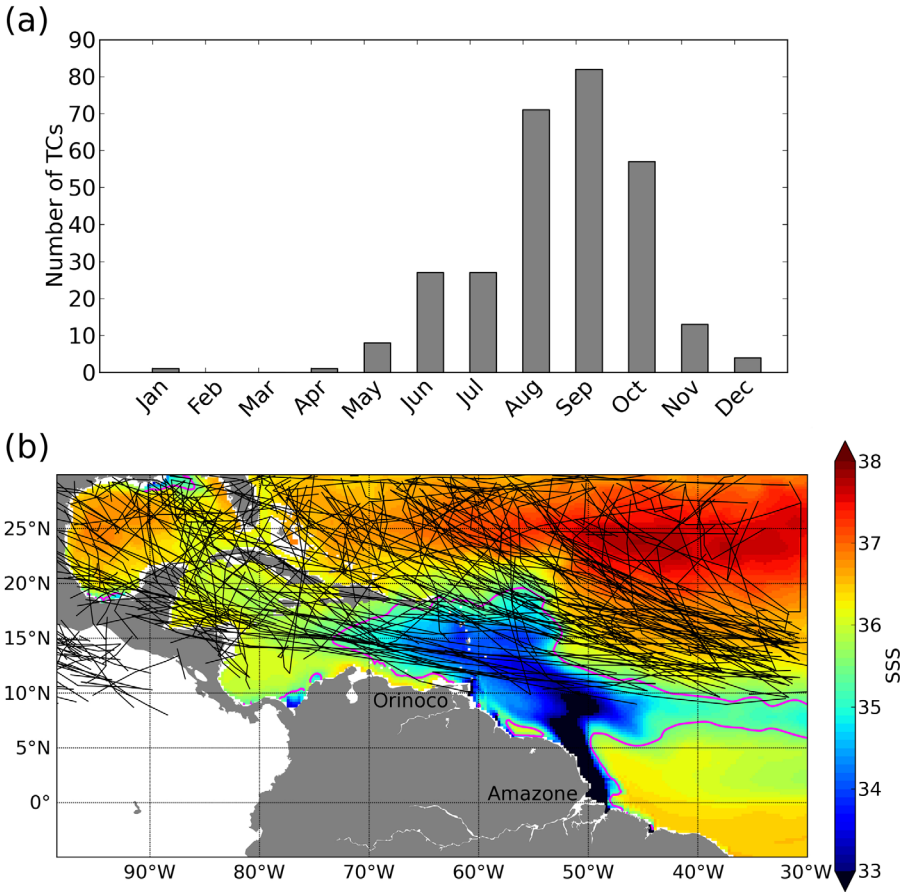

Figure 1. (a) Seasonal evolution of the number of TCS in the Amazon-Orinoco River plume region. (b) Climatological June–November SSS from experiment REF. The magenta curve is the 35.4 sea surface salinity contour. Black lines indicate the cyclones trajectories obtained from the International Best Track Archive for Climate Steward (IBTrACS). All the figures have been made using data from 1998 to 2012.

contributor to the cooling under TCs is mostly the vertical mixing [*Price*, 1981; *Vincent et al*., 2012a], but two other processes are also involved: horizontal/vertical advection that spatially redistributes the temperature, and air-sea fluxes which cool the ocean mainly through latent heat loss and can be dominant for the less intense cyclones [*Vincent et al*., 2012a]. Vertical mixing is modulated by the ocean background conditions. In plume waters, the salinity can contribute significantly to the total density stratification: the analysis by *Maes and O'Kane* [2014] suggest that in the Amazon-Orinoco plume region it could contribute to more than 50% of the upper 300 m averaged stratification. It is thus expected to weaken vertical mixing and TC-induced cooling.

In the Bay of Bengal, *Neetu et al*. [2012] found an influence of freshwater from monsoonal rain and river run-off on the observed TC intensity: on average, they found that haline stratification accounts for 40% of the cooling reduction during post-monsoon season. The barrier layer consists of a salt-stratified layer embedded within the upper, temperature-mixed layer [*Lukas and Lindstrom*, 1991]. At global scale, *Balaguru et al*. [2012a] showed that the rate of intensification of TC is 50% stronger in areas with barrier layers compared to regions without barrier layers. For the Amazon region, *Reul et al*. [2014] found that for the most intense cyclones, cooling is systematically reduced by around 50% over the plume area compared to the surrounding open-ocean waters. They explain these results by the presence of salinity-driven vertical stratification and barrier layer, which reduce the SST cooling in the plume. *Grodsky et al*. [2012] also proposed that barrier layers within the Amazon-Orinoco plume could limit the SST cooling and thus may preserve higher SST and evaporation than outside.

The recent modeling study of *Newinger and Toumi* [2015] analyzes the impact of river freshwater and light absorption by ocean color on ocean temperature and TC response. In contrast to the results mentioned

above, they found a minor effect of the freshwater plume TC-induced cooling amplitude, an effect which is further reduced when accounting for the presence of light-absorbing particles in the upper ocean (which protect the deeper ocean from sunlight, leading to substantial subsurface cooling). In their study, the impact of freshwater on TC-induced cooling is approached using an empirical relationship obtained by *Vincent et al*. [2012b] for the global ocean with relative errors of cooling estimate of order 30% [*Vincent et al*., 2012b].

Owing to these contradictory results regarding the impact of the Amazon-Orinoco river plumes on TC-induced cooling and to our lack of understanding of why the observed cooling in the plume area is weaker than outside [*Reul et al*., 2014], we set up a regional model of the Tropical Atlantic forced with realistic cyclonic winds and analyze the TC cool wake and background conditions obtained from two long-term simulations with and without runoff, inside and outside the plume region. The main objectives of the analysis are 1) to clarify and quantify the impact of the Amazon and Orinoco freshwater flux on the TC response by using a model forced with real cyclones, 2) to detail the processes setting the characteristics of the sea surface cooling induced by tropical cyclones specifically in the region of the Amazon-Orinoco plume and 3) to explain the difference of cooling between the plume region and the open ocean region.

The paper is organized as follows. Section 2 describes the various data sets used in the study and the methodology applied. In section 3, we show the differences of cooling between the plume and open ocean waters for the two model simulations. In section 4, we analyze the processes controlling the observed differences. Finally, results are summarized and discussed in the last section.

2. Data and Methodology

2.1. Regional Model Description

The numerical model is the oceanic component of the Nucleus for European Modeling of the Ocean program (NEMO3.6) [*Madec*, 2014]. It solves the three dimensional primitive equations discretized on a C-grid and fixed vertical levels (z-coordinate). The regional grid of 1/4° horizontal resolution encompasses the Tropical Atlantic (35°S–35°N, 100°W–15°E). It has 75 levels in the vertical, with 12 levels in the upper 20 m and 24 levels in the upper 100 m. A third-order upstream biased scheme (UP3) is used for momentum advection, with no explicit diffusion. A Total Variance Dissipation scheme (TVD) is used for tracers together with a laplacian isopycnal diffusion of 300 $m^2\ s^{-1}$. The temporal integration is achieved by a modified leapfrog Asselin Filter [*Leclair and Madec*, 2009], with a coefficient of 0.1 and a time step of 1200 s.

The vertical diffusion coefficients are given by a Generic Length Scale (GLS) scheme with a k-ε turbulent closure [*Umlauf and Burchard*, 2003], complemented with the type "A" full equilibrium form of *Canuto et al*. [2001] stability functions. A full description of the scheme is given in *Reffray et al*. [2015] and the scheme has already proven its efficiency in regional configuration [e.g., *Maraldi et al*., 2013].

The model is forced at its lateral boundaries with daily outputs from the MERCATOR global reanalysis GLORYS2V3. The open boundary conditions radiate perturbations out of the domain and relax the model variables to 1 day averages of the global experiment. Details of the method are given in *Madec* [2014]. At the surface, the atmospheric fluxes of momentum, heat, and freshwater are provided by bulk formulae [*Large and Yeager*, 2009]. The model is forced with DFS5.2 product [*Dussin et al*., 2014] which is based on ERAinterim [*Dee et al*., 2011] reanalysis and consists of 3 h fields of wind speed, atmospheric temperature and humidity, and daily fields of long wave, short wave radiation and precipitation. DFS5.2 is an update of the product described in *Brodeau et al*. [2010]. The shortwave radiation forcing is modulated on-line by an analytical diurnal cycle. A monthly climatological runoff based on the data set of *Dai and Trenberth* [2002] is prescribed near the river mouths as a surface freshwater flux with increased vertical mixing in the upper 10 m. Note that there is no restoring toward observed or climatological SSS.

The strength of tropical cyclone winds is underestimated in DFS5.2 forcing so synthetic TC winds are superimposed on the DFS5.2 forcing set following the methodology described in *Vincent et al*. [2012a], with a modification. First, the remnant TCs signatures in the original DFS5.2 winds have been filtered out by applying a 11 day running mean to the zonal and meridional wind components, within 600 km around each cyclone track position, with a linear transition from filtered to unfiltered winds between 600 km and 1200 km [*Vincent et al*., 2012a]. Winds reconstructed from analytical TC wind vortex [*Willoughby et al*., 2006]

Table 1. Values of Drag Coefficient (Cd) as a Function of u10

u_{10} (m/s)	10	20	30	40	50
Cd ($\times 10^{-3}$)	1.17	1.78	2.29	1.81	1.35

are superimposed on the filtered wind field at each model time step. The position and maximum wind speed used to build the analytical vortex are obtained from the 6 hourly International Best Track Archive for Climate Steward (IBTrACS) database [*Knapp et al*., 2010] and are temporally interpolated to the model time-step. For wind speeds under 33 m s^{-1} the drag coefficient used in the computation of the wind stress follows the formulation proposed by *Large and Yeager* [2009], but for winds larger than 33 m s^{-1} we applied a decrease of the drag coefficient with increase in the wind speed. The drag coefficient is thus defined as follows:

$$Cd = 10^{-3} * (2.7\,u_{10} + 0.142 + u_{10}/13.09 - 3.14807\,10^{-10} u_{10}^{6}) \text{ for } u_{10} < 33\ \mathrm{m\,s^{-1}} \text{ and}$$

$$Cd = 0.898259/(u_{10}^{2}) + 0.05/u_{10} \text{ for } u_{10} >= 33\ \mathrm{m\,s^{-1}}$$

with Cd the drag coefficient and u10 the wind speed at 10 m (see Table 1). This in order to mimic the observations by *Powell et al*. [2003] which show a reduction of the drag coefficient at very high wind speed. Second, we applied a 25% decrease of the maximum wind speed of the synthetic TCs. This 25% decrease is a simple, ad-hoc method to generate a realistic magnitude of the oceanic cooling in the wake of the TCs, in the model. Indeed, the use of the maximum sustained wind without reduction led to too strong cooling in the wake of TCs. This can be explained by the fact that we make use of circular analytical wind vortex while maximum sustained wind estimates provided by IBTrACS database are generally not representative of the entire cyclone circumference [e.g., *Powell and Houston*, 1998].

The model reference experiment (REF) is initialized with temperature and salinity climatology provided by the WOA98 Atlas from *Levitus et al*. [1998], on 1 January 1979 and is integrated over the period 1979–2012. A twin experiment for which the runoff forcing is removed (NO-RUNOFF) is initialized on 1 January 1995 from the ocean state of REF experiment. Daily averages from 1998 to 2012 are analyzed. We restricted the analysis to this period since satellite SST measurements through clouds are only available from 1998 [*Wentz et al*., 2000].

The various terms contributing to the mixed-layer heat budget are calculated online following *Menkes et al*. [2006]:

$$\partial_t T = -\underbrace{\langle u\partial_x T + v\partial_y T + w\partial_z T\rangle}_{ADV} + \underbrace{\langle D_t(T)\rangle}_{LMIX} + \underbrace{\frac{1}{h}\frac{\partial h}{\partial t}(\langle T\rangle - T_{z=-h}) + \frac{(K_z\partial_z T)_{z=-h}}{h}}_{VMIX} + \underbrace{\frac{Q_{ns} + Q_s(1-F_{z=-h})}{\rho_0 C_p h}}_{FOR}$$

with $\langle . \rangle = \frac{1}{h}\int_{-h}^{0} .dz$ representing depth averaged integration over the variable mixed layer depth.

T is the model potential temperature, (u, v, w) are the velocity components, $D_t(T)$ is the lateral diffusion operator, Kz is the vertical diffusion coefficient for tracers, C_p is the specific heat of sea water, ρ_0 is the surface-referenced density and h is the mixed-layer depth.

Q_{ns} and Q_S are the nonsolar and solar components of the air-sea heat flux and $F_{z=-h}$ is the fraction of the shortwave radiation that reaches the mixed-layer depth. The MLD is defined as the depth where density increase compared to density at 10 m equals 0.03 kg m^{-3}.

The term ADV represents the advection, LMIX is the lateral diffusion, VMIX groups the entrainment and the turbulent flux at the base of the mixed-layer, and FOR is heat flux between the atmosphere and the mixed-layer. In the following, term LMIX is neglected since its contribution is very small. To quantify the relative contribution of all processes to the cooling magnitude, daily averages of each term of the upper-ocean heat budget are integrated over a period starting 10 days prior to TC passage until 3 days after the TC passage as in *Vincent et al*. [2012a].

2.2. Observations

Observed TC trajectories and along-track maximum winds were obtained from IBTrACS [*Knapp et al*., 2010]. Positions and winds are provided every 6 h interval. We averaged these data to have daily positions and winds. The maximum wind speed value of each TC is representative of the 10 min maximum sustained winds at 10 m. In this study we focus on the 1998–2012 period where 291 cyclones (an average of 19

cyclones per year) crossed the study region (5°S–30°N, 100°W–30°W). We define the cyclonic season from June to November, where more than 10 TCs crossed our area each month during the 1998–2012 period over the study region (Figure 1a).

The model mean SST distribution and the amplitude of the cooling in the wake of the TC is compared to Microwave OI SST observations (http://www.remss.com/measurements/sea-surface-temperature/oisst-description) derived from an optimal interpolation of Tropical Rainfall Measuring Mission (TRMM) Microwave Imager (TMI) data and Advanced Microwave Scanning Radiometer AMSR-E data. Daily data from 1998 to 2012 at 0.25° × 0.25° spatial resolution are used.

An updated version of observed SSS fields developed by *Reverdin et al* [2007] is used to describe the salinity distribution. It consists of a compilation of in-situ SSS observations (surface drifters, Argo floats, Prediction and Research Moored Array in the Atlantic (PIRATA) moorings and underway thermosalinographs on research vessels and voluntary merchant ships) objectively mapped on a monthly 1° × 1° grid. These fields have been interpolated linearly onto the 1/4° model grid for comparison.

Monthly fields of salinity and temperature ISAS-13 [*Gaillard*, 2015], available for the period 2004–2012 at 0.25° × 0.25° spatial resolution, are also used. The temperature and salinity fields are reconstructed on 152 levels ranging from 0 to 2000 m depth. They were obtained with ISAS (In Situ Analysis System) version 6 [*Gaillard*, 2012], an optimal estimation tool designed for the synthesis of the Argo global data set [*Gaillard et al*., 2009]. Profiling floats from Argo array is the main data source used in ISAS, but in the tropical Atlantic basin, data from the PIRATA mooring array are also used. For salinity, we adopt the practical salinity scale (pss-78), defining salinity as a conductivity ratio, which does not have physical units.

To validate the model mixed layer depth (MLD) and barrier layer thickness (BLT), we use the MLD climatology and BLT climatology of *de Boyer Montégut et al*. [2004, 2007] at 2° × 2° spatial resolution. As for model MLD, the criterion of MLD used in the observational data set corresponds to the depth at which density differs by 0.03 from the 10 m depth density. These fields have been interpolated linearly onto the model grid to be compared to model outputs.

2.3. Validation of the Cyclonic Season Oceanic State

The mean climatology of observed SST from 1998 to 2012 during the cyclonic season (June–November) is shown in Figure 2a. The main features of the observed SST are well reproduced by the model (Figure 2b), although the model is slightly cooler in the northwestern part of the basin (−0.5°C) and warmer (+1°C) in the Benguela upwelling. We verified that the seasonal cycle of the SST in the region of the Amazon-Orinoco plume is in good agreement with observations (not shown).

The observed spatial distribution of sea surface salinity during the cyclonic season is also well reproduced by the model (Figures 2c and 2d), especially the low salinity plume associated with the Amazon-Orinoco discharge. The June–November mean MLD in the model (Figure 2f) presents a clear south-north gradient in agreement with observations (Figure 2e) [*de Boyer Montégut et al*., 2004]. The MLD shoals to around 20 m in the Amazon plume region, and deepens in the southern hemisphere until 80 m depth. Simulated and observed BLT present the same main pattern, but simulated BLT is thicker by 10 m in the Amazon plume. This might be explained by the lack of data coverage (hashed contours) in the observed product, in this near-shore area. The vertical structure of the salinity and temperature fields will be compared to observations in section 3.

The difference between the experiment without runoff (NO-RUNOFF) and the reference experiment (REF) is presented in Figure 3. As expected, without runoff, SSS is higher in the Amazon-Orinoco plume region, with a difference reaching 3 over a wide area extending north-westward from the Amazon river-mouth. The absence of runoff induces a ML thickening and a BL disappearance, but it has almost no impact on the SST (Figure 3a). This is in agreement with earlier modeling results by *Masson and Delecluse* [2001], *Balaguru et al*. [2012b], *White and Toumi* [2014], *Newinger and Toumi* [2015], who found no significant SST change in response to the presence or absence of large tropical rivers such as the Amazon, Orinoco or Congo rivers. The impact of the barrier layer and haline stratification on the SST could be damped by the fact that we use an ocean model forced through bulk formulae [*Large and Yeager*, 2009], but the weak differences of the net air-sea fluxes in the plume region (weaker than 5 W m^{-2} out of the coastal region) suggest that this potential effect is weak. It is worth noting that with an ocean-atmosphere coupled general circulation model,

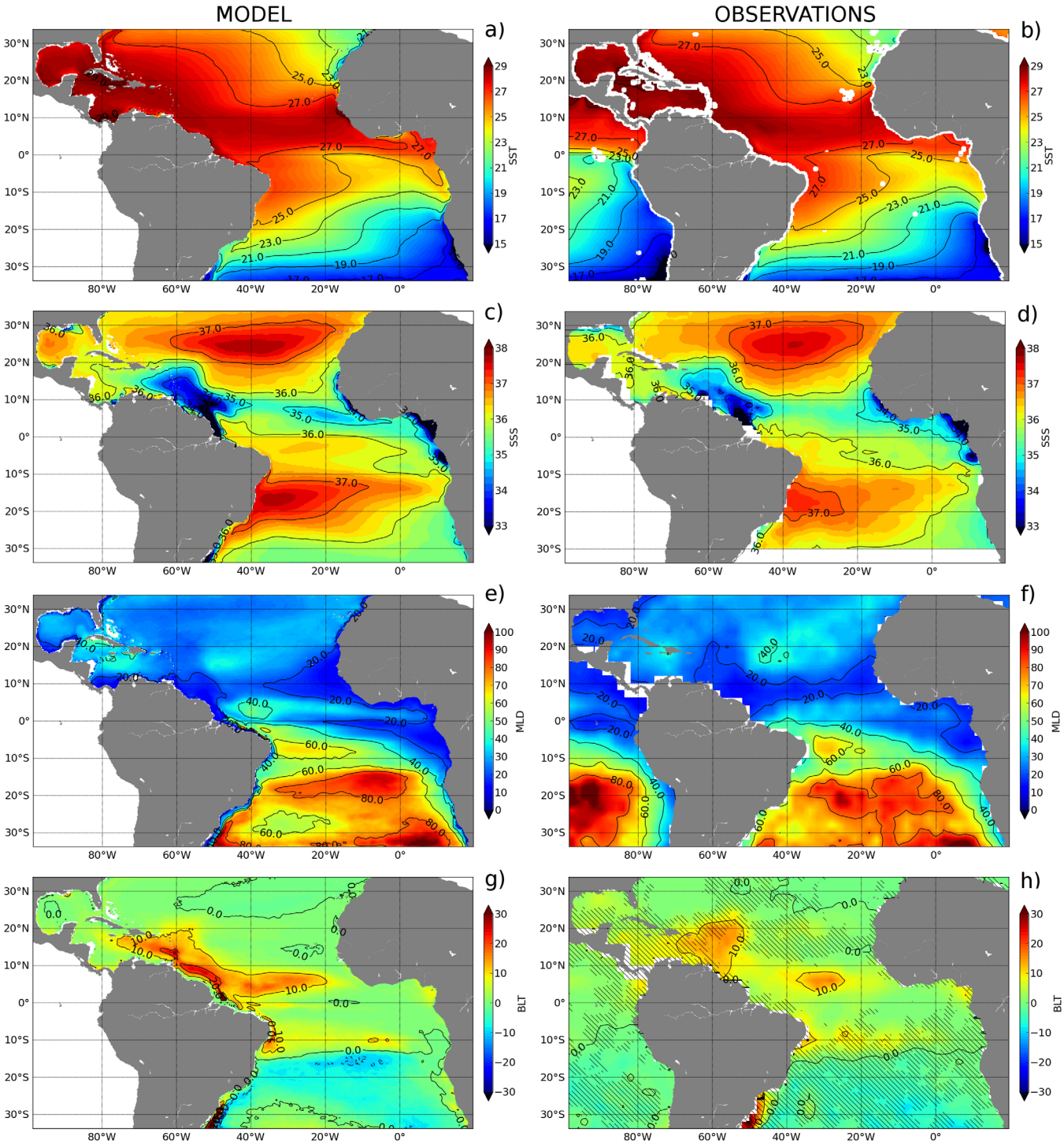

Figure 2. Climatological (a, b) SST (°C), (c, d) SSS, (e, g) MLD (m), and (g, h) BLT (m) averaged from June to November in (left) model and (right) observations averaged from 1998 to 2012 (except the observed MLD and BLT). Observed SST are from OI microwave data set, observed SSS are from *Reverdin et al.* [2007], and observed MLD and BLT are from *de Boyer Montégut et al.* [2004, 2007]. (h) Hashed contours indicate grid points (of 2°×2°) where less than 5 T,S profiles have been used to build the climatology.

sensitivity tests to freshening and increased barrier layer thickness in the Amazon basin did not evidence any significant SST response [*Balaguru et al.*, 2012b].

We can however notice some sensitivity of the SST (and air-sea fluxes) to the absence or presence of run-offs, on coastal waters from the Amazon mouth to the Guajira peninsula (11°N, 72°W). This is due to a slight

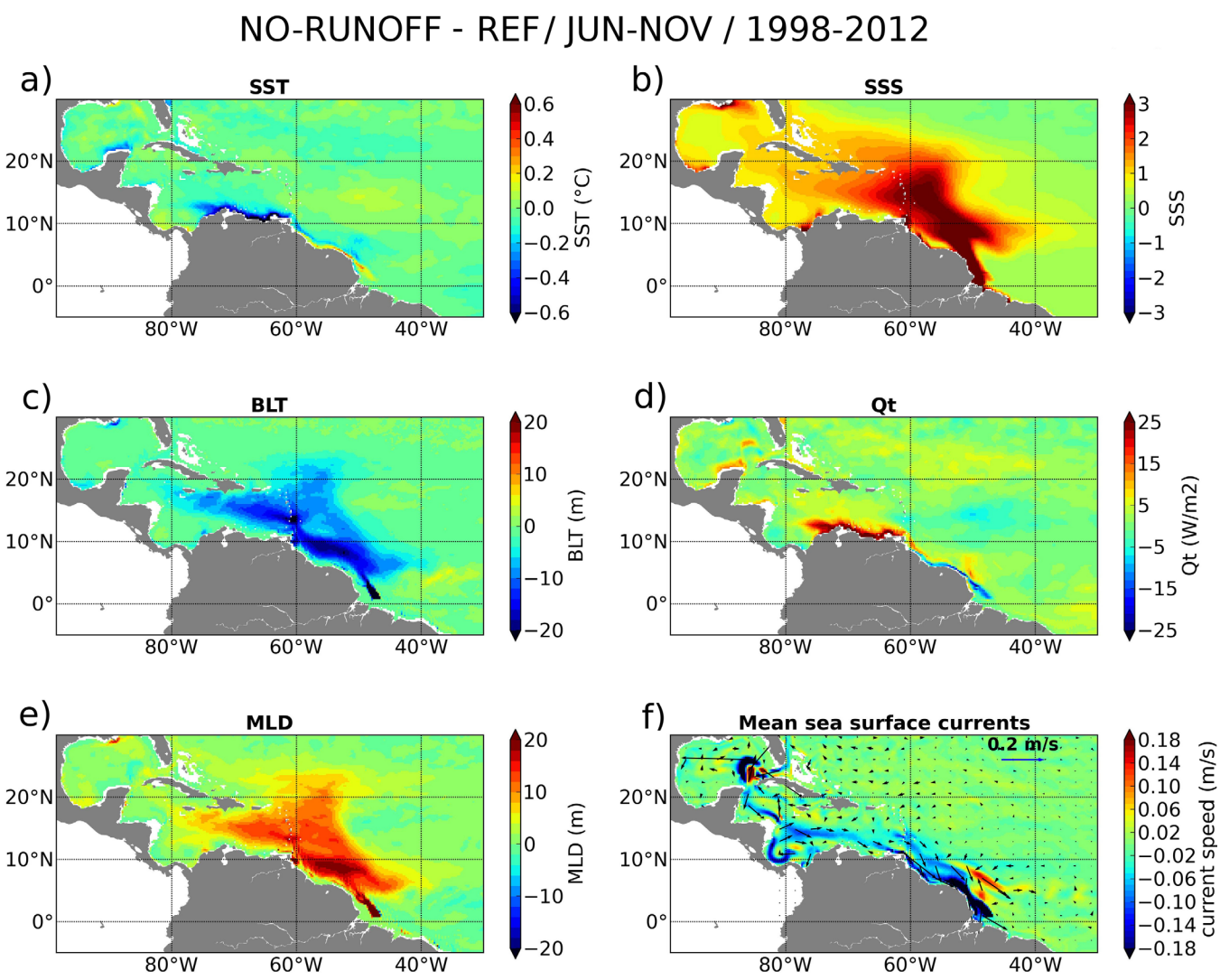

Figure 3. Differences between the model simulation without precipitation (NO-RUNOFF) and the model reference simulation (REF) of June–November averaged (a) SST (°C), (b) SSS, (c) BLT (m), (d) net air-sea heat flux Qt (W m^{-2}), (e) MLD (m), and (f) surface currents (m s^{-1}).

strengthening of the southern american upwelling in response to large scale modification of the pressure gradients and associated currents. This coastal cooling has a very limited off-shore extent (typically 100 km or less), so that it does not enter the TCs-prone area as depicted by Figure 1b. Hence it is not further discussed in the present study.

2.4. Methods

To characterize the ocean response to TCs, we followed the method described in *Vincent et al.* [2012a, 2012b]. First the mean SST seasonal cycle from the various model simulations and observations is subtracted to daily SST data. To characterize the maximum cooling amplitude of the TC, we average SST values within a fixed radius of 200 km around each TC position. The reference unperturbed prestorm SST conditions (SST_0) are defined as the 7 day average from 10 to 3 days before the TC passage. The SST in the cold wake (SST_{CW}) of the TC is defined as the 3 day average starting one day after the storm passage. The maximum amplitude of the SST response in the cold wake (CW) is then defined as $\Delta T_{CW} = SST_{CW} - SST_0$.

To study the influence of the Amazon-Orinoco River plume on the cooling amplitude of a TC, we separate the TCs crossing low salinity waters (referred as "plume waters") from TCs remaining outside the plume area (referred as "open-ocean" waters). A salinity criterion of 35.4, characteristic of the plume horizontal extent (Figure 1b) is used to separate these two regions. The cyclones which trajectory shows a characteristic SSS

(defined as the SSS conditions seen 5 days before the passage of the cyclone, averaged over a radius of 200 km around the cyclone center) below 35.4 are considered as "plume water" cyclones.

We sorted the oceanic response according to 4 different wind categories, following the Saffir–Simpson hurricane wind scale: tropical depressions (TD), tropical storms (TS), category 1 and 2 hurricanes, and category 3 and higher hurricanes. The fourth group comprises all TCs with maximum sustained winds higher than 45 m/s. They are not differentiated in the study since it has been shown that the magnitude of ocean cooling saturates for wind speed higher than 45 m/s [*Vincent et al*., 2012a].

To characterize the ocean background conditions that control the cooling amplitude we computed the Cooling Inhibition index (CI), introduced by *Vincent et al*. [2012b]. This index measures the conversion of kinetic energy to potential energy by vertical mixing, the main process responsible for cooling under TCs [*Vincent et al*., 2012a]. The CI is calculated as:

$$CI = \left[\Delta E_p(-1^\circ\mathrm{C})\right]^{1/3} \text{ with } \Delta E_p(\Delta T) = \int_0^{h_m} (\rho_f - \rho_i(z))\, gz dz$$

where z is the ocean depth, g the acceleration of gravity, ρ_i is the precyclone density profile, ρ_f is the homogeneous final density profile, and h_m is the depth allowing a 1°C surface cooling via an adiabatic mixing [*Vincent et al*., 2012a]. We choose a value of 1°C since the TCs-induced cooling in our region is typically of order 1°C (Figure 5b). The larger the CI, the more stably stratified the pre-TC water column is, and the more difficult it is for a given TC to cool the ocean surface.

To measure the ocean density stratification, we consider various metrics. We use a quantity proposed by *Lloyd and Vecchi* [2011] defined as the depth at which ocean temperature is 2°C below the SST ($H_{(SST-2)}$). We also calculated a CI with constant salinity profile (CI_{SO}), which then only accounts for thermal stratification effect [*Neetu et al*., 2012]. Salinity value for constant profile has been chosen to 36.0, close to the average salinity in the upper 150 m (see Figure 11). To evaluate the impact of salinity stratification (CI_{sal}) we calculated the percentage of CI due to salinity variations: $CI_{sal} = 100.0\ (CI - CI_{SO})/CI$.

Another measure of the degree of stability of the upper ocean is the Brunt-Vaïsäla frequency, N2, which is calculated as a function of vertical profiles of temperature and salinity:

$$N^2 = \frac{-g}{\rho_0}\frac{\partial \rho(T,S)}{\partial z}$$

where ρ_0 is the density, g the gravity. The contributions to the stratification of the vertical distribution of temperature (N_T^2) and salinity only (N_S^2) are computed as follows:

$$N_T^2 = \frac{-g}{\rho_0}\frac{\partial \rho(T,S_0)}{\partial z} \quad , \quad N_S^2 = N^2 - N_T^2$$

with salinity set to a constant value S_0 of 36. We verified that profiles of N^2 are not very sensitive to the value of S_0 used in the calculation. The mean profiles of N^2, N_T^2 and N_S^2 are calculated as an average of the stratification profiles underneath each TC.

3. Results

3.1. Katia Cyclone Case Study

As a first step, we analyze the case study of Hurricane Katia that crossed the Amazon plume in early fall 2011. It was a cyclone that attained its peak intensity as a Category 4 in the Saffir–Simpson hurricane wind scale, with sustained winds reaching 220 km/h. The response to this cyclone was thoroughly documented in *Grodsky et al*. [2012] using satellite and in-situ observations. Its passage left a +1.5 haline wake over the plume region, together with a cool wake of ~1°C that intensified to values larger than 2°C north of the plume. In our simulation, the plume did not extend to the north as in the observations (Figure 4a), but enough so the cyclone trajectory crossed the plume and generated a haline wake of similar amplitude than the observed one (Figure 4a). The cooling distribution is also in good agreement with the observations (Figure 4e). *Grodsky et al*. [2012] suggested that the haline stratification within the plume

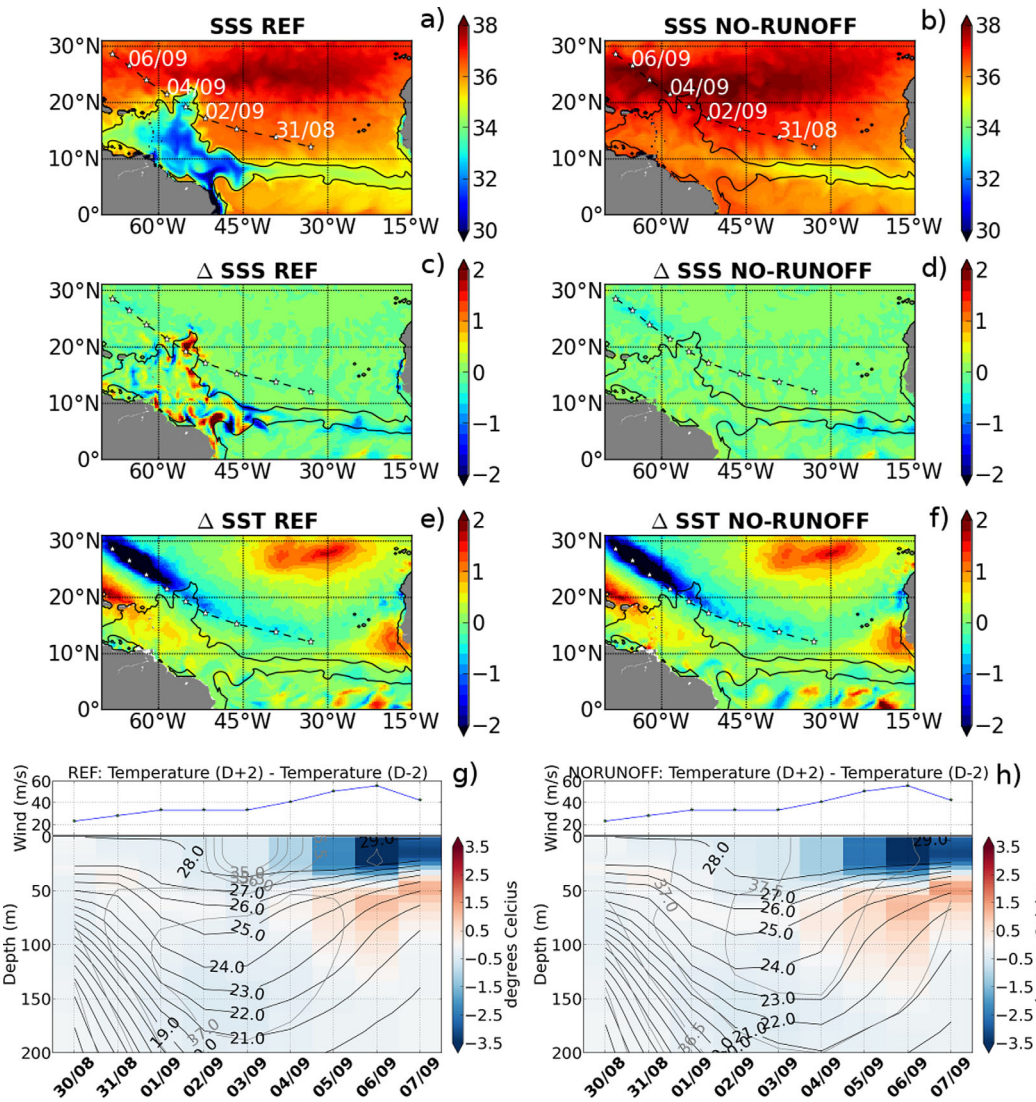

Figure 4. SSS for experiments (a) REF and (b) NORUNOFF at day 30 August 2011 just prior to the development of hurricane Katia. Bullets in white indicate the daily average position of the cyclone. Difference of (c, d) SSS and (e, f) SST between the period just after the passage of Katia (5–10 September) and the period before (25 August to 1 September). The salinity contour 35 is overlaid in order to indicate the position of the river plume. Difference of temperature along the trajectory of the cyclone between two profiles taken 2 days after and 2 days before the passage of the cyclone, for the (g) REF and (h) NORUNOFF experiments. The isotherms (black contours) and isohalines (grey contours) show the oceanic conditions 2 days before the passage of Katia. On top, the evolution of 10 min averaged maximum wind speed is shown.

was responsible for at least 0.5°C weaker SST cooling than outside the plume. In order to test this hypothesis in our simulations, we compare the cool wake in the simulation without river plume (NO-RUNOFF) with the cool wake in the simulation with river plume. In the simulation without plume, there is no more salinization of the surface (Figure 4d), but interestingly the TC-induced cooling remains very close to that observed in *Grodsky et al*. [2012] or to that simulated in presence of river plume. So this suggests that the haline stratification has little impact on the cooling induced by this TC. Instead, the weak cooling over the plume appears to be due at first order to (1) weaker winds over the plume than north of the plume (Figures 4g and 4h), and (2) a larger thermal content in the plume region (which appears to be little affected by the presence or absence of the plume, Figures 4g and 4h). In the following section, we will generalize the analysis of the cool wake to all the TC tracks that have been referenced in the region for the period 1998–2012.

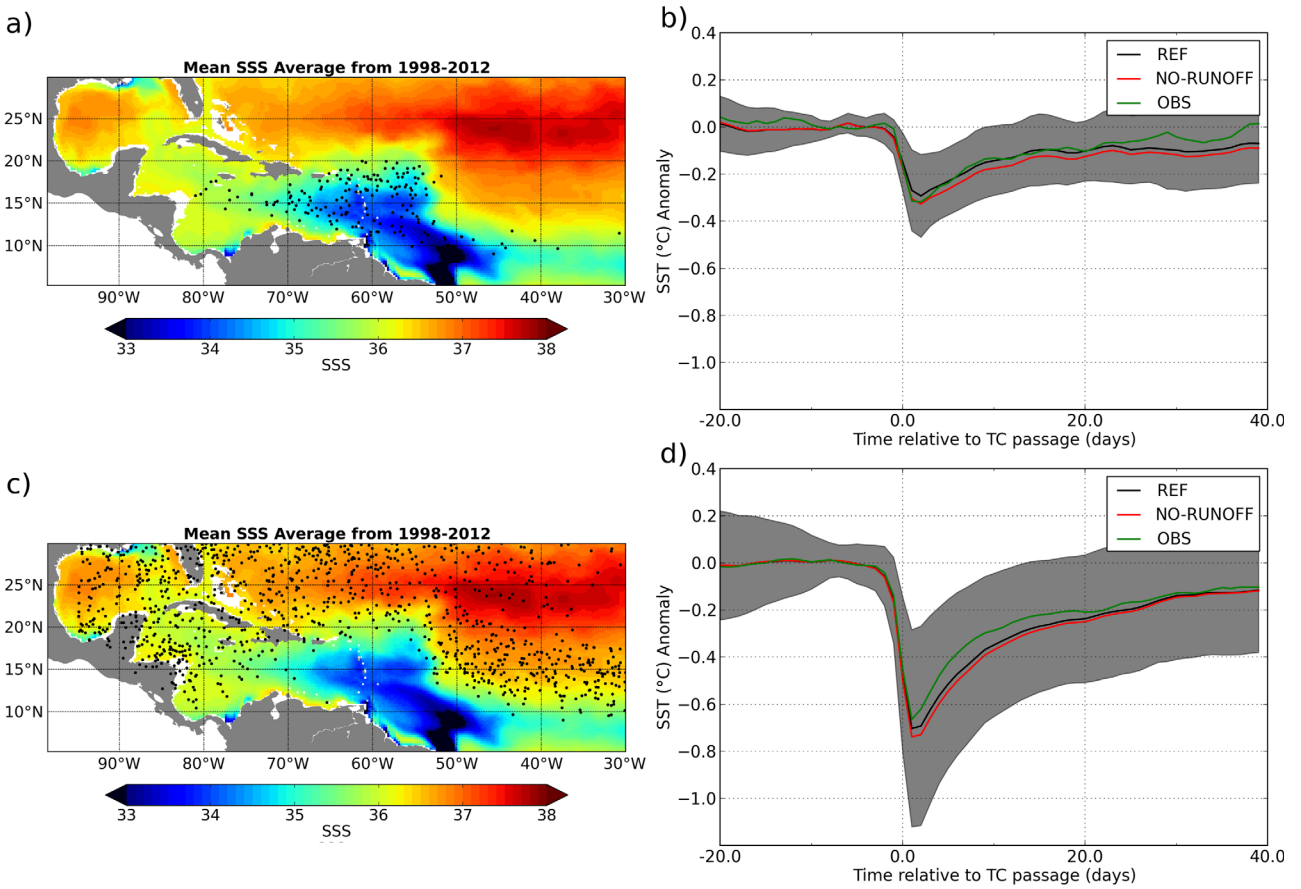

Figure 5. Climatological model SSS from the model during June–November with black dots indicating the daily positions of TC selected in the (a) "plume waters" and (c) "open ocean waters". Temporal evolution of TC-induced SST cooling (in °C) within 200 km of all TCs tracks in model simulations (REF, NO-RUNOFF) and in observations (OBS) in the (b) "plume waters" and (d) "open ocean waters". SST anomalies are calculated with respect to prestorm SST (averaged SST from day-10 to day-3), using the entire 1998–2012 period. Color shading indicates the $^1/_2$ standard deviation around the mean composite value for REF experiment.

3.2. Cooling Amplitude Observed Over the Plume Waters and Open Ocean Waters

The difference of temporal evolution of TC-induced surface cooling is now analyzed within 200 km of all TC tracks over the plume waters (Figure 5a) and the open-ocean waters (Figure 5c). In both cases, the simulation with runoff captures accurately the average observed TC-induced surface cooling (Figures 5b and 5d). SST cooling starts ∼2–3 days before the TC reaches a given location, and the maximum cooling occurs ∼1–2 days after the TC passage. This cooling recedes within ∼ 40 days although the SST remains on average 0.1°C colder than prestorm SSTs, in agreement with previous studies [*Lloyd and Vecchi*, 2011; *Neetu et al*., 2012; *Vincent et al*., 2012a]. For plume waters, the ΔT_{CW} is equal to 0.3°C for both simulation and observations, while for open ocean waters the simulated SST cooling is about 0.7°C and the mean observed cooling is about 0.6°C. So the model response is in good agreement with observations. The distribution of the cooling magnitude as a function of the cyclone category indicates that the model slightly overestimates the cooling for cyclones of category 3 and higher (Figure 6). Nevertheless, these differences are weak compared to the difference of cooling between plume waters and open ocean waters. We cannot expect a perfect agreement between model and observations since the analytical vortices prescribed in the model do not correspond to the structure of each individual cyclone and the oceanic variability at small scales differs between observations and model. Uncertainties regarding the parameterization of the drag coefficient and near-surface mixing due to waves may also contribute to this discrepancy.

Compared to the region out of the plume (which we refer to as open ocean waters), the cooling amplitude in plume waters is reduced by 0.3°C (50%) in observations and 0.4°C (59%) in the model. This reduction increases with the intensity of the cyclone, from 0.47°C for category 1 and 2 to 0.57°C for category 3 and higher in the case of observation. However, in percentage, the ratio of this reduction is slightly higher for hurricanes of

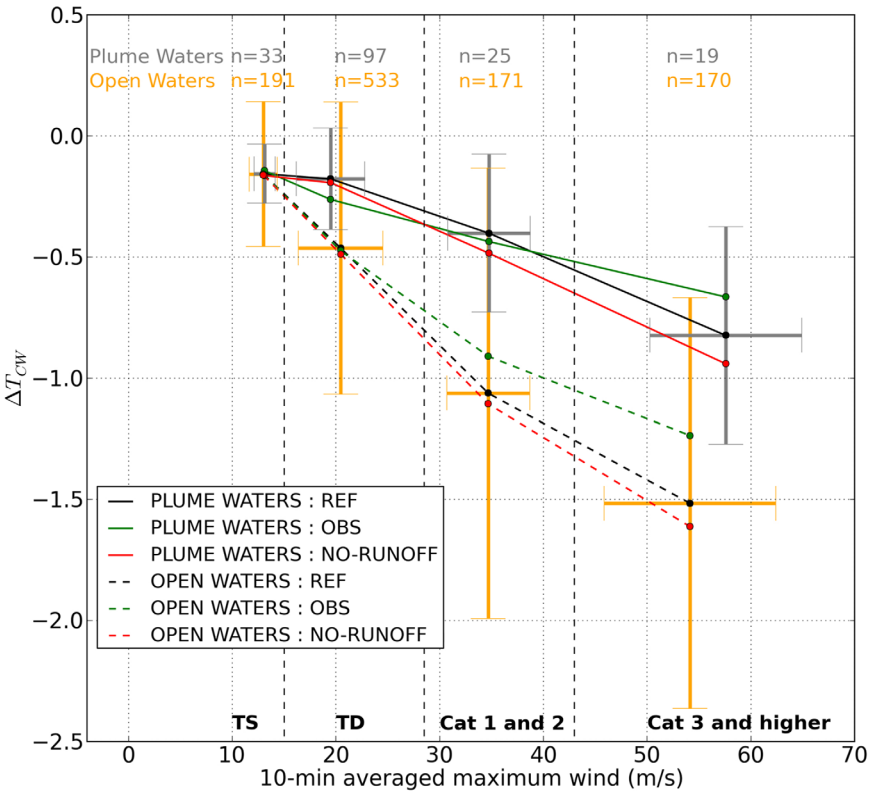

Figure 6. Distribution of mean SST maximum cooling (in °C) as a function of 10 min averaged maximum wind speed (m.s^{-1}) obtained from observations and REF and NO-RUNOFF experiments, using data from the period 1998–2012, for open-ocean waters (dashed lines) and plume waters (continuous line). Four categories of the Saffir Simpson scale (rescaled to 10 min averaged maximum wind speed) are considered: TS, TD, Cat 1 and 2, Cat 3 and higher. Vertical bars indicate the standard deviation of the mean cooling in REF experiment. Horizontal bar indicates the standard deviation of the mean winds.

category 1 and 2 (52% in observations) than for hurricanes of category higher than 3 (46%; see Figure 6 and Table 2). These results are in agreement with those obtained by *Reul et al.* [2014], who found a relative reduction over the plume waters around 35% to 60% depending on the hurricane category.

The cooling over the plume in the experiment without runoff is only ∼0.03°C higher (+11%) than in the experiment with runoff (Figure 5 and Table 2), suggesting that the haline stratification of the Amazon-Orinoco river plume plays only a minor role and does not explain the 0.3–0.4°C or 50% difference of cooling between the plume and the open-ocean waters. In open ocean waters, we do not expect strong differences between the two simulations. Indeed, the SST relative reduction is only around 0.04°C (5%), a difference that can be explained by the salinity transport outside of the region we defined as the plume region (the importance of salinity transport outside of the Amazon-Orinoco plume region has been recently highlighted in *Foltz et al.* [2015] on the basis of observations). In the simulation without runoff, we still have a significant difference

Table 2. ΔT 1: Absolute SST Cooling Difference Between the Plume Waters and Open Ocean Waters and ΔT 2: Absolute SST Cooling Difference Between the Reference Simulation and No-Runoff Simulation

	ΔT 1 (R_A OBS)	ΔT 1 (R_A model REF)	ΔT 1 (R_A model NO-RUNOFF)	ΔT 2 (R_B plume)	ΔT 2 (R_B ocean)
All winds	0.30°C	0.40°C	0.40°C	0.03°C	0.04°C
	(49.6%)	(59.0%)	(56.2%)	(11.2%)	(5.1%)
Cat 1 and Cat 2	0.47°C	0.66°C	0.62°C	0.08°C	0.04°C
	(52.1%)	(62.2%)	(56.3%)	(17.1%)	(4.0%)
Cat >= 3	0.57°C	0.69°C	0.67°C	0.12°C	0.10°C
	(45.7%)	(45.7%)	(41.7%)	(12.5%)	(6.0%)

[a]In parenthesis: Relative reduction of the cooling amplitude between the plume waters and open ocean waters, as R_A= 100 x (ΔSST open ocean - ΔSST plume)/ΔSST open ocean. In the same way, we calculated the relative reduction of the cooling amplitude between model reference simulation and simulation without runoff as, R_B = 100 * (ΔSST NO-RUNOFF - ΔSST REF)/ΔSST NO-RUNOFF.

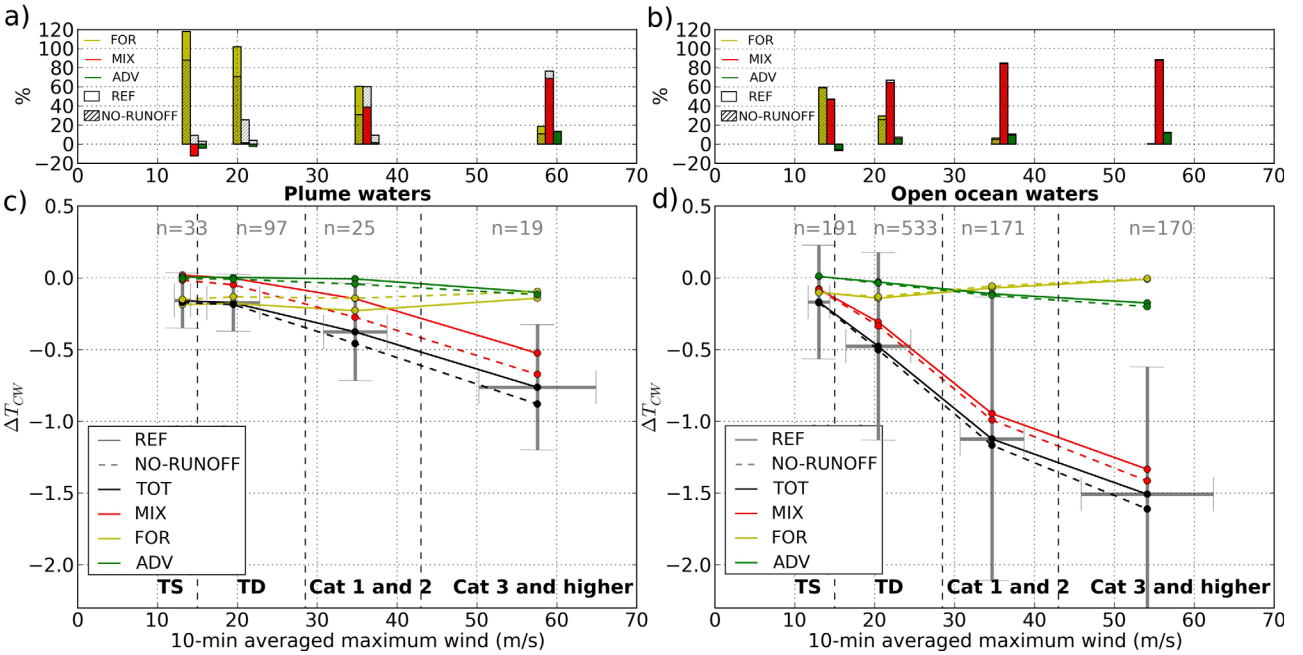

Figure 7. Mean amplitude of TC induced cooling (in °C) and respective contribution of vertical mixing (MIX), heat fluxes (FOR), and advection (ADV) to the total cooling as a function of 4 winds categories of 10 min averaged maximum wind speed (in $m.s^{-1}$) for the (a, c) plume waters and (b, d) the ocean open waters. (c, d) The contributions (in °C) of each process are shown on the bottom and (a, b) the relative contributions (%) of each process in the top. Results for REF are shown with continuous lines and results for NO-RUNOFF are shown with dashed lines.

between the cooling in the plume region and the open ocean (0.4°C, ~56%). The haline stratification and thick BL caused by the river runoff only explains 0.03°C (11%) of the difference in cooling, but not the 0.4°C (40–60%) of SST cooling observed between plume waters and open ocean waters. These results suggest that salinity is not the dominant factor controlling the amplitude of the surface cooling in the plume region, as it has been suggested in recent publications [*Reul et al.*, 2014; *Grodsky et al.*, 2014]. This raises the following question: What can explain the sharp difference of cooling magnitude between plume waters and open ocean waters, since it is not the difference of haline stratification?

3.3. Processes Controlling Differences in Plume and Open Ocean Waters

3.3.1. Upper Ocean Heat Balance

To get further understanding of the processes controlling the observed cooling differences between plume waters and open ocean waters, we analyze in the two regions the contribution of the three main processes responsible for surface cooling: the vertical mixing, the air-sea fluxes and the advection. The relative contribution of each term varies depending on the intensity of the TCs (Figure 7). The contributions are quite similar in the two simulations. For all TCs, advection has a minor impact on the total cooling compared to mixing and surface fluxes.

For weak TCs, surface heat fluxes (mainly latent heat loss, not shown) is the dominant cooling process for upper ocean waters. It accounts for up to 120% of the total cooling in plume waters for TC lower than category 2, and for up to 30% (up to 60% for TS) of the total cooling in open ocean waters for tropical storms and depressions. This process is dominant in plume waters in comparison to open ocean waters for TCs weaker than category 3. In the plume waters, the large contribution of air-sea fluxes to the surface cooling is expected to be due to the weak overall cooling below the cyclones which maintains strong latent heat fluxes.

The contribution of the vertical mixing increases with the intensity of the TCs but is also strongly modulated by the ocean background conditions [*Vincent et al.*, 2012a]. For the most intense TCs (category 3 and higher), vertical mixing is the dominant process that cools the surface: it explains more than 70% of the overall cooling, in agreement with findings by *Vincent et al.* [2012a]. For tropical storms and tropical depressions, it has a much lower contribution and can even act to warm the mixed-layer in the river case (this is

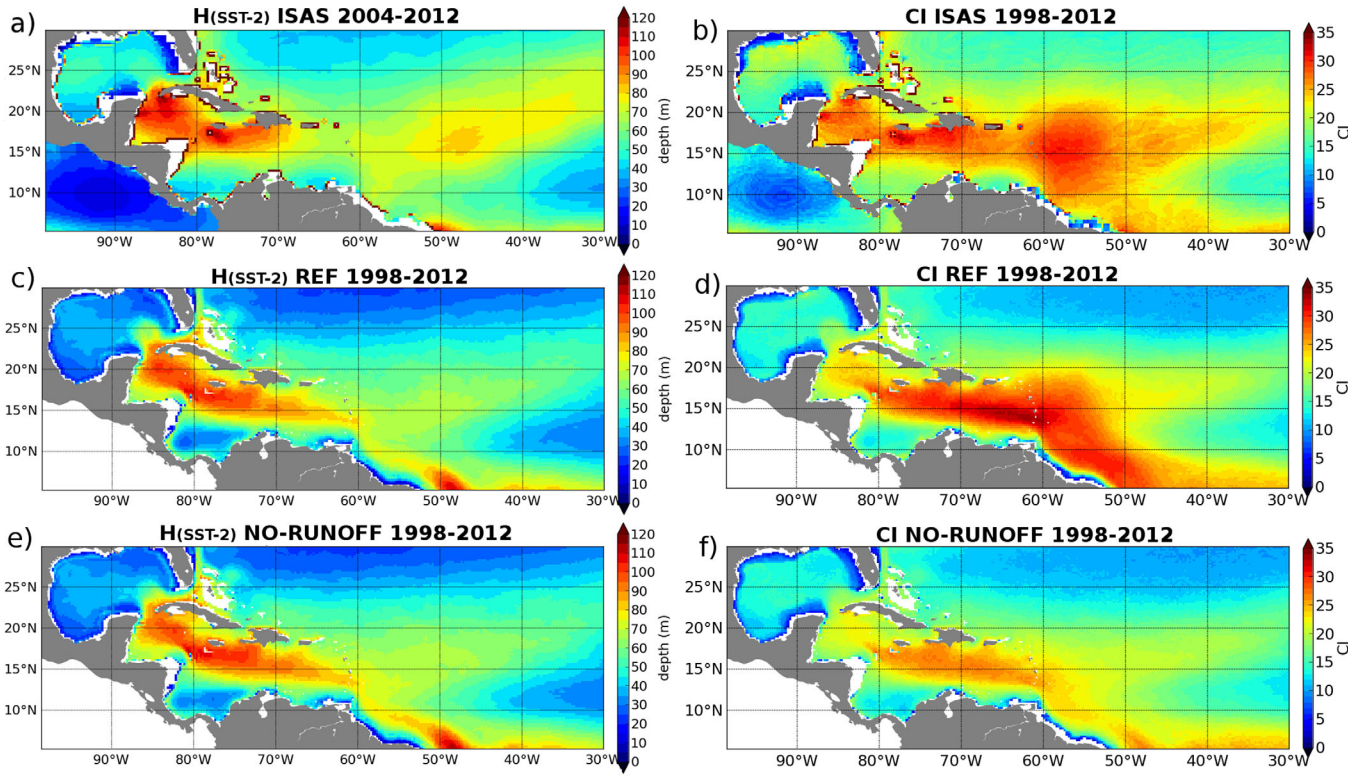

Figure 8. Depth at which the ocean temperature is 2°C below the SST ($H_{(SST-2)}$ in m) and Cooling Inhibition Index (CI in $(J/m^2)^{1/3}$) calculated from (a, b) ISAS observations, (c, d) REF simulation and (e, f) NO-RUNOFF simulation from June to November during the period 1998–2012.

the signature of thermal inversions that are supported by the haline stratification). Interestingly we note that the contribution of the vertical mixing to the total cooling is weaker in the plume region than in open ocean waters, leading to large overall differences of cooling between the two regions. The purpose of the following section is to explain why such a difference exists.

3.3.2. Analysis of the Oceanic Background Conditions

A key quantity to assess differences between plume and open waters cooling is $H_{(SST-2)}$, the depth at which the subsurface temperature is 2°C lower than the surface temperature. Average values are shown in Figure 8 for model and observations, for the period June–November from 1998 to 2012. To first order, model and observations display the same pattern showing a strip of deep $H_{(SST-2)}$ between 10°N and 20°N from 80°W to 40°W, viz. over part of the Atlantic Warm Pool [*Wang and Enfield*, 2001]. The largest fraction of the Amazon-Oricono plume coincides with this zone of deep $H_{(SST-2)}$. This indicates that the thermal structure of the ocean in the plume region predisposes the plume waters to a TC-induced cooling weaker than outside. Moreover we note that $H_{(SST-2)}$ is very much alike in both simulations, suggesting that the river runoff has a weak impact on this quantity.

The distribution of $H_{(SST-2)}$ is in good agreement with the depth of the isotherm 23°C (D23, Figure 9). The east to west deepening of the D23 in the latitudinal band 10°N–25°N (Figure 9a), which comprises a large part of the Amazon-Orinoco river plume, occurs at first order as a linear response to the wind stress curl of the trade winds (Figure 9b). This has been verified by applying a long Rossby wave linear model [*Kessler*, 2006] to the Tropical Atlantic. Such model has been mainly used to analyze low frequency (seasonal) variability in the Tropical Pacific [e.g., *Meyers*, 1979]. The model is forced with seasonally varying climatological wind stress computed from the DFS5.2 forcing set over the period 1998–2012, and climatological D23 obtained from the experiment REF is used as eastern boundary condition. The thermocline depth inferred from the Rossby model is shown in Figure 9c for the period June–November. It accounts for the major features of observed and modeled D23 and $H_{(SST-2)}$ shown in Figures 8 and 9, in particular the east to west deepening of the D23 in the band 10°N–25°N. This indicates that the deep thermal structure in the plume region and associated large value of CI are to first order wind-driven.

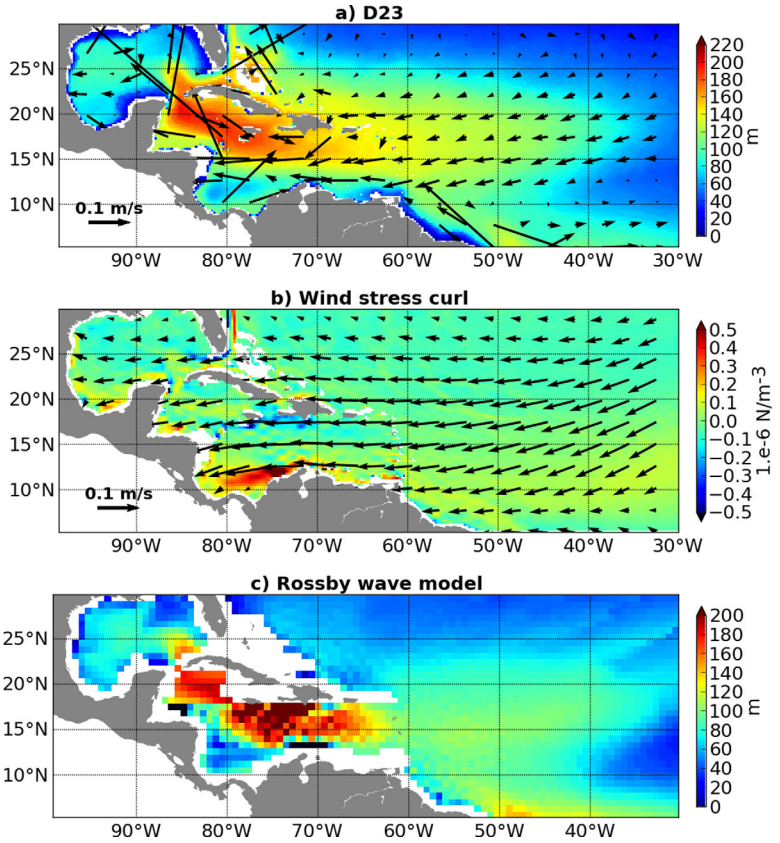

Figure 9. (a) Depth of the 23°C isotherm (D23, in m), (b) wind stress curl (N m^{-3}) of the trade winds and (c) thermocline depth (m) estimated from the long Rossby wave linear model averaged from June to November during the period 1998–2012. (a) Currents (m/s) between 100 and 200 m are superimposed to D23 and (b) winds stress (N/m^2) is superimposed to winds stress curl. The Rossby model is similar to the one described in *Kessler* [2006]. We used a gravity wave speed c=2 m/s and a damping time scale of 18 months.

The analysis of the Cooling Inhibition index (CI) provides further understanding of the impact of the background oceanic conditions that lead to the observed and modeled cooling difference between plume and open ocean waters. Indeed, contrary to $H_{(SST-2)}$ discussed in previous paragraph, this quantity accounts both for temperature and salinity contribution to the overall density stratification of the upper ocean. In both model and observations, CI index presents high values (> 25 $(J/m^2)^{1/3}$) over an extended area of the plume between 80°W and 60°W, in the same region of deep thermal stratification observed previously (Figures 8b and 8d). The average of the CI underneath TCs in plume waters and open-ocean waters for different ΔT ranging from 0 to 3°C is shown in Figure 10 and Table 3. It shows that for $\Delta T > 0.5$°C, the CI in the plume waters is about 10 $(J/m^2)^{1/3}$ larger than in open water. This is in agreement with the large difference of cooling observed (of 0.3–0.4°C) due to vertical mixing between plume and open ocean waters.

Simulation without runoff presents slightly lower CI values than the reference simulation, around 20% lower in plume regions and 10% lower in open ocean areas (Figure 8f) but these values remain important and higher than 20 $(J/m^2)^{1/3}$. This suggests that thermal stratification is more important in this area than haline stratification, a result in accordance with the difference of TC-induced surface cooling obtained previously between the reference simulation and simulation without runoff.

In order to quantify the contribution of the salinity to the CI, CIso accounting only for thermal stratification is shown in Figure 10b and the percentage of CI due to salinity is shown in Figure 10c. Like the value of CI, CIso is always higher in plume waters than open-ocean waters. Moreover values of CIso are close to values of CI, suggesting again that thermal stratification plays the main role in the observed cooling. The percentage of CI due to salinity (Figure 10c), considering 1°C of surface cooling, represents about 30% of the total CI. In the simulation without runoff, the percentage of CI due to salinity is around 11%. Although the freshwater input by the rivers is removed, there is still a salinity stratification in the upper ocean layers, due to

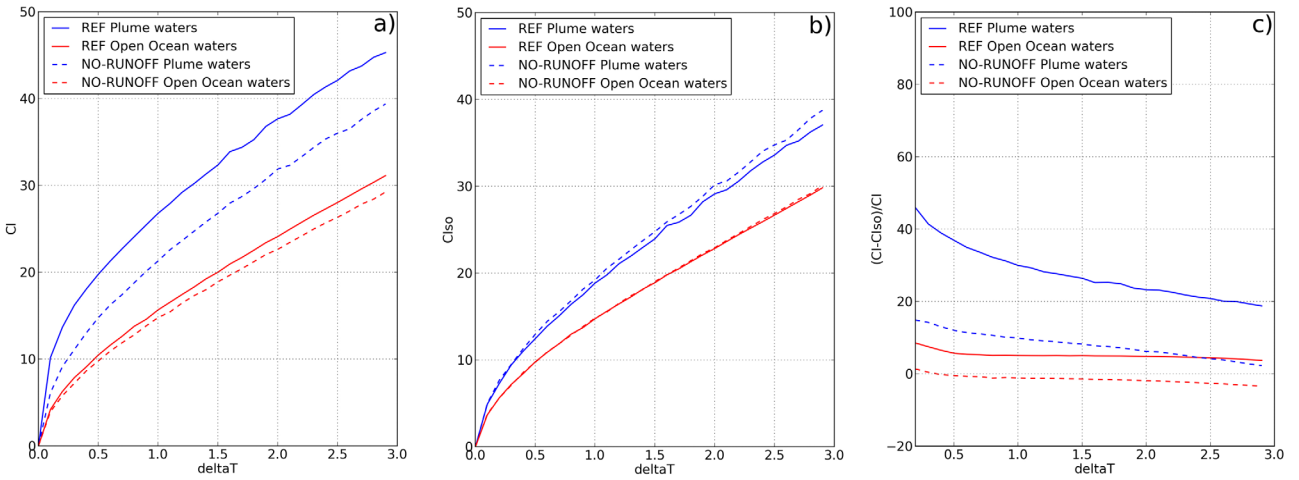

Figure 10. (a) CI (in $(J/m^2)^{1/3}$), (b) Clso (in $(J/m^2)^{1/3}$) and (c) percentage of CI due to salinity (CI_{sal}) as a function of SST cooling, computed using the background conditions of simulations REF (continuous line) and NO-RUNOFF (dashed line). CI was calculated underneath each TC in a radius of 200 km and averaged over the plume waters and open ocean waters.

air-sea freshwater fluxes and/or salinity advection. So the impact on the CI (assuming 1°C of surface cooling) of salinity stratification induced by runoff only is of about 20%. We note that the contribution of the salinity to the CI decreases when ΔT increases (Figure 10c). This suggests that the impact of the salinity on the cooling inhibition is weaker for the stronger TCs.

4. Summary and Discussion

4.1. Summary

In this paper, we investigate the impact of salinity stratification and barrier layer on the TC-induced cooling amplitude in the Amazon-Orinoco plume region. We analyze a regional ocean numerical simulation forced by realistic TC winds over the 1998–2012 period, when high-quality satellite SST data are also available. During these 15 years, 291 cyclones crossed the study region. A careful comparison with observations shows that the simulation represents realistically the ocean background state and the sea surface temperature response to TCs.

In order to infer the impact of the low-salinity surface waters we first analyze the difference in TC-induced cooling amplitude between plume waters and open ocean waters. Compared to open ocean waters, TC-induced cooling amplitude in plume waters is reduced on average by 0.4°C (0.7°C for the strongest cyclones) in both model and observations, representing a reduction of order ∼50%. An analysis of the contribution of the various processes controlling the cooling reveals that for TCs weaker than category 2, air-sea exchanges control the cooling in plume waters and contribute significantly for open ocean waters. For TCs of category 3 and higher, vertical mixing explains the main part of the cooling for both plume waters and open ocean waters. The vertical mixing is directly related to the ocean background conditions. The CI, which measures the ocean "resistance" to cooling [*Vincent et al.*, 2012a] is found significantly higher in plume waters than in open ocean waters. However, one question arose: Is this observed difference of cooling magnitude and of CI directly due to the Amazon-Orinoco runoff?

Table 3. Mean CI (in $(J/m^2)^{1/3}$) Calculated Underneath Each Cyclones Positions (Over a Radius of 200 km) in the Plume Waters and in the Open Waters

	Mean CI in the Plume 1998–2012	Mean CI Open Waters 1998–2012
REF	27.1 ± 4.4	17.8 ± 5.4
NO-RUNOFF	22.0 ± 3.6	16.7 ±4.8
Nb of cyclones positions	174	1065

In order to answer this question we compared two simulations with and without runoff forcing, in order to isolate the effect of salinity stratification and barrier layer. Compared to the simulation with runoff, the simulation without runoff does not show any significant change of the seasonal SST. This rules out the role of freshwater input by the Amazon and Orinoco rivers, in accordance with previous studies [*Masson*

and Delecluse, 2001; *White and Toumi*, 2014; *Newinger and Toumi*, 2015]. Moreover TC-induced SST cooling is very similar in both simulations with only a slightly higher cooling (+0.03°C) in the plume region for the simulation without runoff.

This sensitivity study suggests that the haline stratification and thick barrier layers caused by the river runoff may explain only 11% (0.03°C) of the 0.4°C average difference of SST cooling observed between plume waters and open ocean waters, and that the thermal stratification is at leading order, the environmental factor explaining the difference of TC induced cooling between the plume and the open waters. We found that the presence/absence of the plume has a weak influence on the difference in thermal stratification between these two regions. Instead, the occurrence of the large CI, deep $H_{(SST-2)}$ in the plume region are related to a deep 23°C isotherm in this region, well explained as a linear response to the trade winds wind stress curl, consisting of the superposition of local Ekman pumping and propagation of a low frequency seasonal Rossby wave. The weak influence of the plume is confirmed by an evaluation of the percentage of CI due to salinity which shows that salinity stratification does not account for more than 30% of the total CI, while thermal stratification account for more than 70% of the total CI.

Note that in the plume region, about one third of the 30% of the salinity contribution is not due to runoff but to other processes (air-sea freshwater fluxes and advection), as suggested by the difference between REF and NORUNOFF in Figure 10c. Salinity stratification due to runoff does not account for more than 20% in the total CI.

4.2. Discussion

Are our results consistent with previous studies of the impact of salinity and barrier layers on the TC-induced cooling amplitude in the Amazon-Orinoco plume region?

As discussed in the introduction, recent studies suggested that the freshwater input from the Amazon and Orinoco rivers could be an active player in the intensification of tropical cyclones [*Balaguru et al*., 2012a; *Grodsky et al*., 2012; *Maes and O'Kane*, 2014; *Reul et al*., 2014]. From a comparison of TC-induced surface cooling between plume and open ocean waters, *Reul et al*. [2014] suggested that haline stratification is the main responsible for the difference in surface cooling between the two regions. *Balaguru et al*. [2012a] showed that the rate of intensification of tropical cyclones is 50% stronger in areas with BL compared to regions without BL. *Vizy and Cook* [2010] showed that forcing a model with warm SST anomalies over the plume region increases the number of Atlantic basin storms by 60%, but did not demonstrate that rivers are causing warm anomalies. *Grodsky et al*. [2012] also proposed that BL regions within the Amazon-Orinoco plume could limit the SST cooling and thus may preserve higher SST and evaporation than outside. Through the analysis of a simulation without runoff and without BL, our model also shows that the Amazon-Orinoco freshwater plume acts to inhibit the cyclones-induced cooling (in line with these past studies). However, in stark contrast with the past studies, we show that this effect is minor as, to the first order, the differences in cooling between the plume region and open ocean waters are not due to the salinity stratification differences, but to thermal stratification differences.

Other papers analyzed the role of the salinity stratification by computing the haline and thermal part of the Brunt-Vaïsäla frequency (N^2) in the upper ocean pycnocline. By analyzing N^2 from observations, *Maes and O'Kane* [2014] determined that the ocean salinity stratification in the Amazon-Orinoco plume region contributes to 40–50% to N^2 as compared to thermal stratification, over the upper 300 m. Indeed, if we calculate an average of N^2, N_S^2 and N_T^2 taken underneath each TC (Figure 11) we obtained similar results: salinity strongly contributes to the total stratification. In the simulation without runoff, we obtain a low contribution of the salinity to the stratification (weak values of N_S^2), as expected. Note that small gradient of salinity persists probably due to advection and local evaporation-precipitation balance. These profiles illustrates that the maximum of total stratification is not the key variable to explain changes in TC ocean response. Our results indicate that they have a weak influence in modulating the sea surface cooling induced by the tropical cyclones: although the maximum stratification is more than twice higher in the reference simulation (1.7 cph) than in NO-RUNOFF simulation (0.7 cph), the TC-induced cooling is similar.

The rate of deepening of the mixed-layer depth h_t can be estimated [see e.g., *Cushman-Roisin*, 1981] as $h_t = 2\rho_0 m u^{*3}/g\Delta\rho h_{ml}$, with ρ_0 the background density, m a coefficient which depends on the fraction of the water column that is affected by mixed-layer convection events, u^* the friction velocity, h the mixed-layer depth and $\Delta\rho$ the difference of density between the mixed-layer depth and the ocean below. This formulation

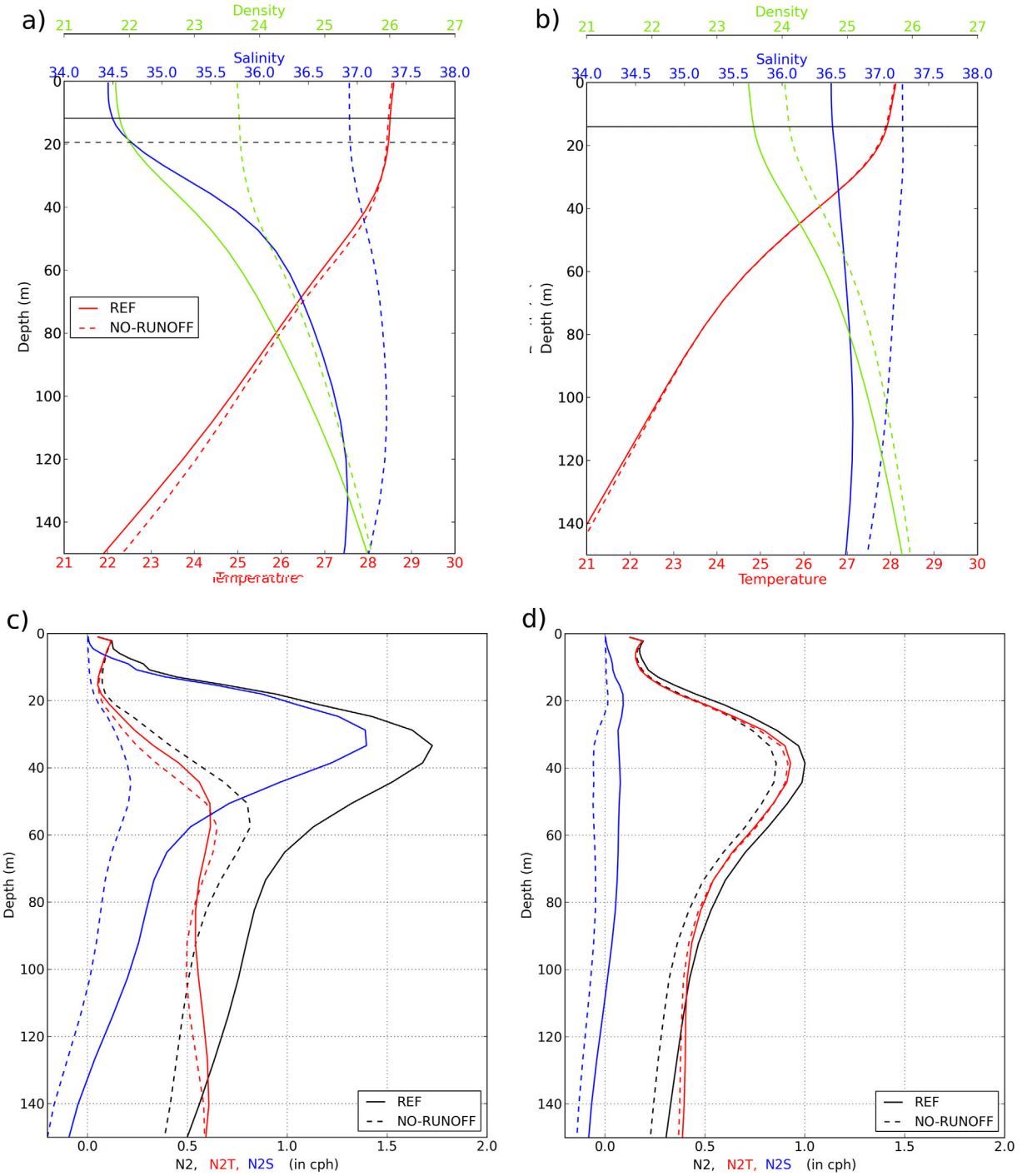

Figure 11. (a, b) Mean temperature (°C), salinity, and potential density relative to reference pressure (kg m^{-3}) profiles calculated underneath each TCs and corresponding to the conditions seen 5 days before the passage of the cyclone. Horizontal lines in Figures 11a and 11b indicate the mean mixed layer depth. Note that in Figure 11b both dashed and continuous horizontal lines are superimposed, indicating that the mean mixed layer depth in the open ocean region is equal in both experiments. (c, d) Mean profiles of N^2, N_T^2, and N_S^2 (in cph) calculated underneath each TCs in (a, c) plume waters and(b, d) open ocean waters.

illustrates that for a given wind the deepening rate is inversely proportional to $\Delta\rho$ and to the mixed-layer depth. As illustrated in Figure 11, the difference of density between the mixed-layer depth and the ocean below (the density of this is taken as the mean density between the bottom of the mixed-layer and 100 m) is twice larger in the river case ($\Delta\rho$ = 21.8–23.2 = 1.4 kg m^{-3} in the river case, and $\Delta\rho$ = 23.6–24.3 = 0.7 kg m^{-3} in the no-river case). But note that at the same time, the mixed-layer depth is twice larger in NO-RUNOFF (h_{ml}=∼20 m)

compared to REF (h_{ml}=~10 m). So both effects almost compensate and lead to similar deepening rate. This is consistent with our main result that haline stratification has only a weak effect of the hurricane cool wake.

To have a clearer view of the respective roles of temperature and salinity stratification in the observed cyclone-induced cooling, we implemented a simplified *Kraus and Turner* [1967] mixed layer model and we solved it successively for the two contrasted cases of thermal stratification characterizing the plume area (deep thermocline) and the open ocean area (shallow thermocline), under forcing conditions characteristic of an average (viz. category 2) hurricane, for a variety of salinity stratification conditions (see Appendix A). This simplified model successfully reproduced the order of magnitude of cooling simulated by the OGCM, hereby confirming that the basic mechanisms at stake in the present study are essentially one-dimensional. Consistently with past studies, the simplified model confirmed that under a given temperature stratification, the cyclone-induced cooling is more important when the salinity stratification below the mixed layer is weaker. But while "REF" and "NO-RUNOFF" OGCM experiments could be seen as two extreme cases in terms of salinity stratifications in the plume region, our simplified model confirmed that the thermal stratification conditions are the dominant factor explaining the contrasted cyclone-induced cooling patterns across our area of interest, whatever the salinity stratification conditions one can reasonably think of. It also suggested that the background barrier layer thickness is not a first order parameter for the control of the magnitude of the cyclone-induced cooling. The simplified model also confirmed the prominent role of air-sea heat loss below the cyclone, that significantly distorts the basic mechanism invoked in the past studies (stronger salinity stratification inducing weaker cooling) based on mechanical considerations only.

Our results are in good accordance with those obtained by *Newinger and Toumi* [2015]. These authors found that the freshwater plume from Amazon and Orinoco rivers does not change significantly the seasonal SSTs. Furthermore, by analyzing the CI in simulations with and without runoff, they found that freshwater plume does not significantly change the CI, with a difference of only 4.3 $(J/m^2)^{1/3}$, close to the 5 $(J/m^2)^{1/3}$ difference we found between REF and NO-RUNOFF in plume waters. However, the authors inferred (indirectly from a vertical mixing cooling parameterization based on the CI) a difference of cooling between simulations with and without runoff of around 0.2°C for the stronger TCs. As detailed in *Vincent et al*. [2012b], a limitation of the CI definition and associated parameterization is that it only considers TC-induced cooling driven by penetrative vertical mixing, whereas air-sea fluxes also play a significant role for weak TCs. Through the analysis of modeled upper ocean heat budget, we quantified the different processes controlling the cooling. For the plume region, we show that air-sea fluxes contribute significantly to the cooling (>80% for cyclones of category 2 and below and ~30% for cyclones of category 3 and higher), which further stresses that vertical mixing alone cannot explain the cooling (on average it contributes 30% to the cooling). This explains why we found that the plume contributes 20% to CI but only 11% for SST cooling inhibition. This suggests that CI parameterization may not be completely adapted to the plume region. This could explain that we found a weaker sensitivity of TC cooling to runoff (~0.1°C) than *Newinger and Toumi* (~0.2°C). Thus, with equivalent difference in CI between the two experiments, while directly taking into account the cyclones in the model, we found no major differences in the observed TC-induced cooling.

As discussed by *Vincent et al*. [2012a], an improvement of the model horizontal resolution could improve the realism of the present results. They reported that a 1/2° horizontal resolution model was enough to capture the transfer of cyclone kinetic energy to the upper ocean, so the mixing induced by this injection of energy, together with the modification of the air-sea fluxes, allow to reproduce a statistically realistic cooling. However at such low resolution (and also at the resolution of 1/4° as we use in this study), some processes that could influence the cooling are poorly or even not resolved. First, the downward penetration of the near inertial energy, which is a source of mixing at depth, is strongly dependent of the model horizontal and vertical resolutions (e.g., *J. Jouanno et al*., 2016). Second, we miss restratification processes associated with submesoscale circulation that develop in the wake of the cyclone [*Huang and Oey*, 2015]. The relevance of these processes in controlling the amplitude of the cooling remains to be investigated.

Finally, in the present study we quantified the influence of temperature and salinity on the total observed TC-induced cooling. Our results show that the effect of runoff and barrier layers on the TC-induced SST cooling only leads to a 10% weakening of the cooling. This percentage could be further reduced by the effect of light absorbing particles in the plume [*Newinger and Toumi*, 2015]. Thus Amazon and Orinoco river plumes do not seem to control the amplitude of the cool wake, which stands in contrast with recent publications [*Balaguru et al*., 2012a; *Grodsky et al*., 2012; *Maes and O'Kane*, 2014; *Reul et al*., 2014]. Instead, we found that temperature related mixed-

layer depth and depth of the thermocline (both being closely linked in this region) may play the main role in explaining the observed differences in CI and cooling between the plume and open ocean waters. This result is in agreement with *Neetu et al.* [2012], who found that thermal stratification explains most of the seasonal variability of the cooling inhibition in the Bengal Bay, a region that also undergoes important river discharges. It is worth mentioning that this study does not allow to conclude on the overall influence of the Amazon and Orinoco river plumes on TCs development. The modulation of the seasonal SSTs by the river plumes may have an impact on the regional background atmospheric conditions so it could influence the formation and intensification of TCs as already suggested by *Ffield* [2007].

Our results were obtained in a region characterized by the largest freshwater source into the world oceans. Indeed, in the plume region, between 70°W–45°W and 2°S–20°N, the annual runoff represents ∼70% of the annual freshwater input to the ocean and the percentage of precipitation only reaches ∼30% (mainly due to the ITCZ). Thus, our conclusion that haline stratification due to river plumes has weak impact on TC-induced surface cooling, should apply for other plumes in the tropical oceans.

Appendix A: Sensitivity of Cyclone-Induced Cooling to Temperature and Salinity Stratification in an Idealized Mixed-Layer Model

The objective of this section is to shed light on the respective roles of temperature and salinity stratifications on cyclone-induced cooling, using a simplified version of the *Kraus and Turner* [1967, hereinafter KT] mixed layer model (see e.g., *Jourdain et al.* [2013] for an application of a similar model to TC-induced cooling). It consists of a one-dimensional framework, illustrated on Figure A1. Before the arrival of the cyclone, we assume salinity and temperature are completely mixed in the upper water column, down to the mixed layer depth (MLD_0) and to the isothermal layer thickness (ILT_0), respectively. The mixed layer being thinner than the isothermal layer, a barrier layer exists, with thickness BLT_0. Below the upper mixed layer, the profiles follow a linear stratification, with slope $-a$ for temperature and b for salinity:

$$T = T_0 \text{ in the isothermal layer} \tag{A1}$$

$$T = T_0 - a(z - ILT_0) \text{ in the thermocline layer} \tag{A2}$$

$$S = S_0 \text{ in the isohaline layer} \tag{A3}$$

$$S = S_0 + b(z - ILT_0 - BLT_0) \text{ in the halocline layer} \tag{A4}$$

We assume that the cyclone deepens the mixed layer by entrainment of the underlying (cooler) thermocline water, and that this entrainment takes the form of an adiabatic mixing. Hence we neglect any viscous dissipation of momentum in the entrainment process, so that the input of kinetic energy E by the hurricane wind stirring is entirely transformed into potential energy. Once the entrainment is completed, the mixing is assumed to be perfect (homogeneous profiles of temperature and salinity) down to the new isothermal layer thickness ILT_1. For simplicity we assume the barrier layer has been entirely eroded in the process.

The conservation of heat yields:

$$T_1 \times ILT_1 = T_0 \times ILT_0 + \int_{ILT_0}^{ILT_1} [T_0 - a(z - ILT_0)]dz \tag{A5}$$

From the transformation of kinetic energy into potential energy, one can write:

$$E = \int_{ILT1}^{0} (\rho_1(z) - \rho_0(z))gzdz \tag{A6}$$

where ρ_1 and ρ_0 are the profiles of density after and before the cyclone pass, respectively.

For a given kinetic energy input E, we solve equation (6) iteratively to compute ILT_1, using the *Jackett and McDougall* [1995] equation of state. Then equation (5) allows computing T_1, which yields the cyclone-induced cooling:

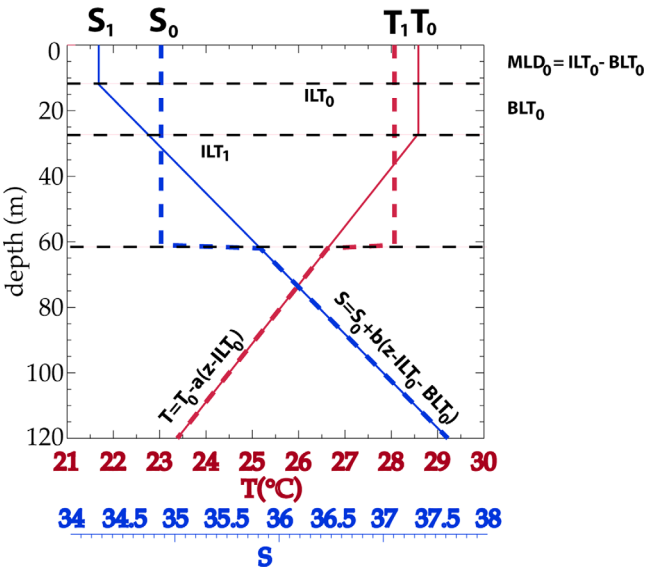

Figure A1. Examples of idealized salinity (blue) and temperature (red) profiles used in our simplified mixed layer model. Solid lines show the profiles before the cyclone, dashed lines show the resulting profiles after cyclone-induced mixing. Mixed layer depth (MLD), isothermal layer thickness (ILT) and barrier layer thickness (BLT) are indicated before (subscript "0") and after (subscript "1") mixing. The equations of temperature and salinity profiles beneath the homogeneous layer are also indicated.

$$T_{CW} = T_1 - T_0 \quad \text{(A7)}$$

The ocean response is analyzed for 4 cases with stratification parameters similar to the model profiles in plume and open ocean waters, with or without runoff forcing.

We impose the following value for the kinetic energy input:

$$E = 2.10^3 J.m^{-2}$$

This can be seen as representative of the mechanical energy needed to generate the cooling produced by a cyclone of category 2. This value is representative of the mean kinetic energy transfered to the ocean by TCs [see e.g., *Vincent et al.*, 2012b, their Figure 6]

For the sake of simplicity, we solve our idealized model for two different temperature stratifications, mimicking the two contrasted cases analyzed with the OGCM:

1. case "deep thermocline": $ILT_0 = 28m$; this value is typical of the plume waters area (see Figure 11a)
2. case "shallow thermocline": $ILT_0 = 14m$; this value corresponds to the open ocean area (see Figure 11b)

In both cases, the initial ML temperature T_0 is fixed as follows:

$$T_0 = 28^\circ C$$

$$a_{deep\ thermocline} = 5, 5.10^{-2\circ} C.m^{-1}$$

$$a_{shallow\ thermocline} = 7, 0.10^{-2\circ} C.m^{-1}$$

These are reasonable assumptions, as can be seen on all profiles of Figure 11 ("REF" as well as "NO-RUNOFF" experiments).

For each of these two temperature stratifications, we vary independently the background barrier layer thickness BLT_0 (from 0 to 14 m thickness) as well as the salinity stratification slope b (from 0 to 0.03 m^{-1}), and we compute the cooling predicted by the KT model for each couple of these two parameters (BLT_0, b). Figure A2 presents the cyclone-induced cooling we obtain as a function of these two independent parameters, for the "deep thermocline" case (Figure A2a) and for the "shallow thermocline" case (Figure A2b). For both cases, the magnitude of the cyclone-induced cooling decreases when the background barrier layer thickness increases. Similarly, the magnitude of the cooling decreases when the strength of the salinity stratification in the halocline increases. This is true for both cases of thermal stratification ("deep thermocline" and "shallow thermocline"), and for all regimes of salinity stratification we considered. However, the sensitivity of the cooling to background barrier layer thickness is very weak in the "shallow thermocline" case, the magnitude of the cooling depending primarily on the strength of the halocline stratification. In the "deep thermocline" case, the sensitivity of the cooling to barrier layer thickness is larger when the halocline stratification is larger (more than 1.5×10^{-2} m^{-1}). For moderate halocline stratification (less than 1.5×10^{-2} m^{-1}), the cooling depends on the halocline stratification only, as in the "shallow thermocline" case. Such sensitivity appears to be consistent with the mechanisms proposed by *Grodsky et al.* [2012] and *Reul et al.* [2014]. However, beyond this sensitivity of the cooling to salinity stratification parameters, we note that the most striking contrast in cooling magnitude is seen when comparing the two different cases of thermal stratification ("deep thermocline" and "shallow thermocline"). Indeed, whatever the values of background barrier layer thickness BLT_0 and halocline stratification b one can reasonably think of in our area, the

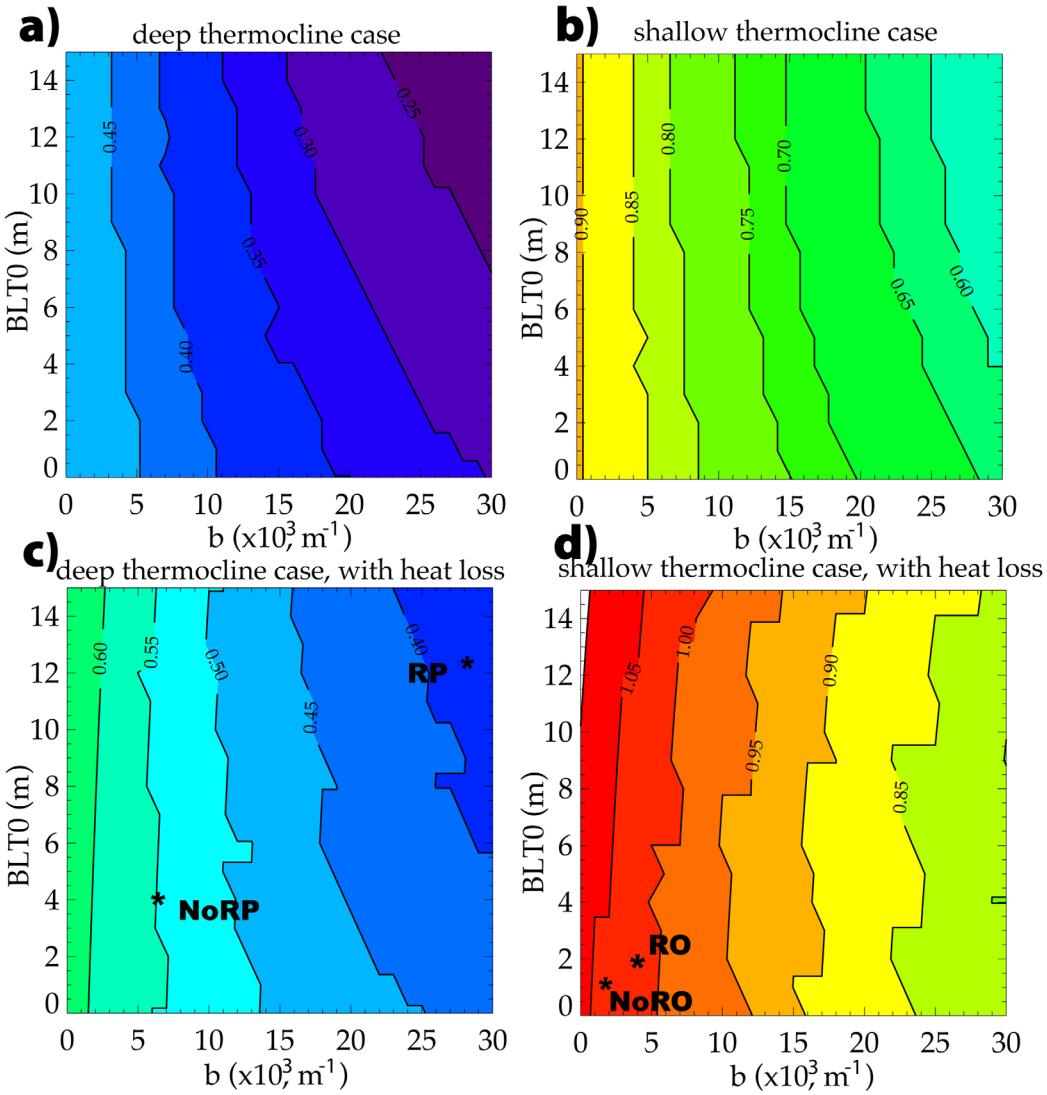

Figure A2. Cyclone-induced cooling predicted by the simplified KT model (in °C), as a function of salinity stratification in the halocline (x axis, in m^{-1}) and background barrier layer thickness (y axis, in m): response obtained for the (a, c) "deep thermocline" case and (b, d) "shallow thermocline" case (see the text for details). Isocontours every 0.05°C. (a,b) KT model forced by cyclonic wind stirring only. (c, d) KT model forced by cyclonic wind stirring and cyclonic heat flux. The black stars on Figures A2c and A2d feature the cyclone-induced cooling predicted by the KT model for the four situations discussed in section 3 with the OGCM: REF experiment in Plume waters (RP), NO-RUNOFF experiment in Plume waters (NoRP), REF experiment in Open ocean waters (RO), NO-RUNOFF experiment in Open ocean waters (NoRO).

difference of cooling magnitude between the two cases ("deep thermocline" versus "shallow thermocline") typically amounts to 0.40°C, which is dominant over the contrasts of cooling magnitude seen within any of these two cases (typically within 0.15°C of their mean value).

In order to improve the realism of our KT model, we incorporated the effect of atmospheric heat fluxes on the cyclone-induced cooling, as they were found to be important in our OGCM experiments (see section 3.3). For the two different thermal stratification cases ("deep thermocline" and "shallow thermocline"), a heat loss of 2.10^7 $J.m^{-2}$ is imposed during the cyclone event. This value is typical of the values we diagnosed from the broad range of cyclones imposed to the OGCM simulation, for the various conditions we considered ("REF" simulation, "NO-RUNOFF" simulation, plume area or open ocean area, see Figure 7). Figure A2(cd) presents the cyclone-induced cooling predicted by the modified KT model, again for the two different thermal stratification cases ("deep thermocline" on Figure A2c and "shallow thermocline" on Figure A2d). As expected, with this additional heat loss, the magnitude of the cyclone-induced cooling is increased compared to the case with mechanical forcing only (Figures A2a and A2b), for all the stratification regimes. Interestingly, the sensitivity of

the cyclone-induced cooling to the halocline stratification is reduced (with isocontours less tightly spaced) compared to the case of the KT model with mechanical forcing only (Figures A2a and A2b). This is particularly true for strong salt-stratification conditions (in excess of 1.5×10^{-2} m^{-1}). In the shallow thermocline case (Figure A2d), the magnitude of the cooling is basically independent of the background barrier layer thickness, revealing the compensating effect of adiabatic processes (mixing) and diabatic processes (heat loss to the atmosphere): a thick barrier layer inhibits the cooling by mixing but at the same time it induces a thin mixed layer that is more prone to cooling by heat fluxes.

Figures A2c and A2d also displays the cooling predicted by the KT model, for the temperature and salinity stratifications defining the four contrasting situations discussed in section 3 for our OGCM (see Figure 11). Our simplified KT physics reasonably reproduces the magnitude of the cooling simulated by the OGCM, with typical errors inferior to 0.1°C. This confirms that the mechanisms we identified in section 3 to explain the different behavior of the OGCM in the four different scenarii (plume versus open ocean, "REF" simulation versus "NO-RUNOFF" simulation) can be reasonably explained by this simplified KT one-dimensional physics. In particular, it appears quite clearly that the difference of cyclone-induced cooling simulated by the OGCM in the plume area in REF experiment (label "RP" on Figure A2cd) versus for the "NO-RUNOFF" experiment (label "NoRP" on Figures A2c and A2d), is significantly weaker when the full forcing is considered (wind stirring and heat flux) than in conditions where the KT model forcing is mechanical only (wind stirring) (see Figure A2a and A2b). This tends to confirm the important role of cyclone-induced heat loss in shaping the ocean response to cyclone forcing.

Acknowledgments
This study was supported by EU FP7/2007-2013 under Grant Agreement No. 603521, project PREFACE. Computing facilities were provided by GENCI project GEN7298. We aknowledge the ISAS team for making freely available the temperature and salinity climatology. Sea surface salinity data derived from thermosalinograph instrumentsinstalled onboard voluntary observing ships were collected, validated, archived, and made freely available by the French Sea Surface Salinity Observation Service (http://www.legos.obs-mip.fr/observations/sss/). We acknowledge discussions with G. Reffray, R. Bourdalle-Badie, G. Madec, J. Vialard, G. Samson, and S. Jullien.

References

Balaguru, K., P. Chang, R. Saravanan, L. R. Leung, Z. Xu, M. Li, and J.-S. Hsieh (2012a), Ocean barrier layers effect on tropical cyclone intensification, *Proc. Natl. Acad. Sci. U. S. A.*, *109*(36), 14,343–14,347.

Balaguru, K., P. Chang, R. Saravanan, and C. J. Jang (2012b), The barrier layer of the Atlantic Warmpool: Formation mechanism and influence on the mean climate, *Tellus, Ser. A. 64*, 18162, doi:10.3402/tellusa.v64i0.18162.

Brodeau, L., B. Barnier, A.-M. Treguier, T. Penduff, and S. Gulev (2010), An ERA40-based atmospheric forcing for global ocean circulation models, *Ocean Modell.*, *31*(3–4), 88–104.

Canuto, V. M., Howard, A., Y. Cheng, and M. S. Dubovikov (2001), Ocean turbulence. Part I: On point closure model–momentum and heat vertical diffusivities, *J. Phys. Oceanogr.*, *31*(6), 1413–1426.

Chiang, T.-L., C.-R. Wu, and L.-Y. Oey (2011), Typhoon Kai-Tak: An ocean's perfect storm, *J. Phys. Oceanogr.*, *41*(1), 221–233, doi:10.1175/2010JPO4518.1.

Cushman-Roisin, B. (1981), Deepening of the wind-mixed layer: A model of the vertical structure, *Tellus*, *33*, 564–582, doi:10.1111/j.2153-3490.1981.tb01782.x.

Dai, A., and K. E. Trenberth (2002), Estimates of freshwater discharge from continents: Latitudinal and seasonal variations, *J. Hydrometeorol.*, *3*, 660–687.

de Boyer Montégut, C., G. Madec, A. S. Fischer, A. Lazar, and D. Iudicone (2004), Mixed layer depth over the global ocean: An examination of profile data and a profile-based climatology, *J. Geophys. Res.*, *109*, C12003, doi:10.1029/2004JC002378.

de Boyer Montégut, C., J. Vialard, S. S. C. Shenoi, D. Shankar, F. Durand, C. Ethé, and G. Madec (2007), Simulated seasonal and interannual variability of mixed layer heat budget in the northern Indian Ocean, *J. Clim.*, *20*, 3249–3268, doi:10.1175/JCLI4148.1.

Dee, D. P., et al. (2011), The ERA-Interim reanalysis: Configuration and performance of the data assimilation system, *Q. J. R. Meteorol. Soc.*, *137*, 553–597, doi:10.1002/qj.828.

Dussin, R., B. Barnier and L. Brodeau (2014), The making of Drakkar forcing set DFS5, *DRAKKAR/MyOcean Rep. 05-10-14*.

Ffield, A. (2007), Amazon and Orinoco River plumes and NBC Rings: Bystanders or participants in hurricane events?, *J. Clim.*, *20*, 316–333.

Foltz, G. R., C. Schmid, and R. Lumpkin (2015), Transport of surface freshwater from the equatorial to the subtropical North Atlantic Ocean, *J. Phys. Oceanogr.*, *45*(4), 1086–1102, doi:10.1175/JPO-D-114-0189.1.

Gaillard, F. (2012), ISAS-Tool version 6: Method and configuration, doi:10.13155/22583.

Gaillard, F. (2015), ISAS-13-CLIM temperature and salinity gridded climatology, *Sismer*, doi:10.12770/e23e19d4-dc4d-40d1-8cfd-4e9f70746dd7.

Gaillard, F., E. Autret, V. Thierry, P. Galaup, C. Coatanoan, and T. Loubrieu (2009), Quality control of large argo datasets, *J. Atmos. Oceanic Technol.*, *26*, 337–351.

Grodsky, S. A., N. Reul, G. S. E. Lagerloef, G. Reverdin, J. A. Carton, B. Chapron, Y. Quilfen, V. N. Kudryavtsev, and H.-Y. Kao (2012), Haline hurricane wake in the Amazon/Orinoco plume: AQUARIUS/SACD and SMOS observations, *Geophys. Res. Lett.*, *39*, L20603, doi:10.1029/2012GL053335.

Grodsky, S. A., G. Reverdin, J. A. Carton, and V. J. Cole (2014), Year-to-year salinity changes in the Amazon plume: Contrasting 2011 and 2012 Aquarius/SACD and SMOS satellite data, *Remote Sens. Environ.*, *140*, 14–22, doi:10.1016/j.rse2013.08.033.

Huang, S.-M., and L.-Y. Oey (2015), Right-side cooling and phytoplankton bloom in the wake of a tropical cyclone, *J. Geophys. Res. Oceans*, *120*, 5735–5748, doi:10.1002/2015JC010896.

Jackett, D. R., and T. J. McDougall (1995), Minimal adjustment of hydrographic data to achieve static stability, *J. Atmos. Oceanic Technol.*, *12*, 381–389.

Jouanno, J., X. Capet, G. Madec, G. Roullet, P. Klein, and S. Masson (2016), Dissipation of the energy imparted by mid-latitude storms in the Southern Ocean, *Ocean Sci. Discuss.*, doi:10.5194/os-2016-3, in review.

Jourdain, N., M. Lengaigne, J. Vialard, G. Madec, C. Menkes, E. Vincent, S. Jullien, and B. Barnier (2013), Observation-based estimates of surface cooling inhibition by heavy rainfall under tropical cyclones, *J. Phys. Oceanogr.*, *43*, 205–221, doi:10.1175/JPO-D-12-085.1.

Kessler, W. S. (2006), The circulation of the eastern tropical Pacific: A review, *Prog. Oceanogr.*, *69*(2–4), 181–217, doi:10.1016/j.pocean.2006.03.009.

Knapp, K. R., M. C. Kruk, D. H. Levinson, H. J. Diamond, and C. J. Neumann (2010), The International Best Track Archive for Climate Stewardship (IBTrACS): Unifying tropical cyclone best track data, *Bull. Am. Meteorol. Soc.*, *91*, 363–376, doi:10.1175/2009BAMS2755.1.

Kraus, E., and J. Turner (1967), A one dimensional model of the seasonal thermocline II: The general theory and its consequences, *Tellus*, *19*, 98–106.

Large, W. G., and S. Yeager (2009), The global climatology of an interannually varying air-sea ux data set, *Clim. Dyn.*, *33*, 341–364, doi: 10.1007/s00382-008-0441-3.

Leclair M., and G. Madec (2009), A conservative leapfrog time stepping method, *Ocean Modell.*, *30*, 88–94.

Levitus, S., T. P. Boyer, M. E. Conkright, T. O' Brien, J. Antonov, C. Stephens, L. Stathoplos, D. Johnson, and R. Gelfeld (1998), NOAA Atlas NESDIS 18, World Ocean Database 1998: 1: INTRODUCTION, 346 pp., U.S. Gov. Print. Off., Washington, D. C.

Lloyd, I. D., and G. A. Vecchi (2011), Observational evidence for oceanic controls on hurricane intensity, *J. Clim.*, *24*(4), 1138–1153, doi: 10.1175/2010JCLI3763.1.

Lukas, R., and E. Lindstrom (1991), The mixed layer of the western equatorial Pacific Ocean, *J. Geophys. Res.*, *96*(S01), 3343–3357, doi: 10.1029/90JC01951.

Madec, G. (2014), "NEMO ocean engine" (Draft edition r5171), *Note du Pôle de modélisation 27*, Inst. Pierre-Simon Laplace, France, ISSN No 1288-1619.

Maes, C., and T. J. O'Kane (2014), Seasonal variations of the upper ocean salinity stratification in the Tropics, *J. Geophys. Res. Oceans*, *119*, 1706–1722, doi:10.1002/2013JC009366.

Maraldi C., et al. (2013), NEMO on the shelf: Assessment of the Iberia–Biscay–Ireland configuration, *Ocean Sci., 9, 745-771*, doi:10.5194/os-9-745-2013.

Masson, S., and P. Delecluse (2001), Influence of the Amazon river runoff on the tropical Atlantic, *Phys. Chem. Earth, Part B*, *26*, 137–142.

Meyers, G. (1979), On the annual Rossby wave in the tropical North Pacific Ocean, *J. Phys. Oceanogr.*, *9*, 633–674.

Menkes, C. E., J. G. Vialard, S. C. Kennan, J. P. Boulanger, G. V. Madec (2006), A modeling study of the impact of tropical instability waves on the heat budget of the eastern equatorial Pacific, *J. Phys. Oceanogr.*, *36*, 847–865.

Mignot, J., C. de Boyer Montégut, A. Lazar, and S. Cravatte (2007), Control of salinity on the mixed layer depth in the world ocean: 2. Tropical areas, *J. Geophys. Res.*, *112*, C10010, doi:10.1029/2006JC003954.

Neetu, S., M. Lengaigne, E. M. Vincent, J. Vialard, G. Madec, G. Samson, M. R. Ramesh Kumar, and F. Durand (2012), Influence of upper-ocean stratification on tropical cyclone-induced surface cooling in the Bay of Bengal, *J. Geophys. Res.*, *117*, C12020, doi:10.1029/2012JC008433.

Newinger, C., and R. Toumi (2015), Potential impact of the colored Amazon and Orinoco plume on tropical cyclone intensity, *J. Geophys. Res. Oceans*, *120*, 1296–1317, doi:10.1002/2014JC010533.

Pailler, K., B. Bourlès, and Y. Gouriou (1999), The barrier layer in the western tropical Atlantic Ocean, *Geophys. Res. Lett.*, *26*, 2069–2072.

Powell, M. D., and S. H. Houston (1998), Surface wind fields of 1995 Hurricanes Erin, Opal, Luis, Marilyn, and Roxanne at landfall, *Mon. Weather Rev.*, *126*, 1259–1273.

Powell, M. D., P. J. Vickery, and T. A. Reinhold (2003), Reduced drag coefficient for high wind speeds in tropical cyclones, *Nature*, *422*, 279–283, doi:10.1038/nature01481.

Price, J. F. (1981), Upper ocean response to a hurricane, *J. Phys. Oceanogr.*, *11*, 153–175.

Reffray, G., R. Bourdalle-Badie, and C. Calone (2015), Modelling turbulent vertical mixing sensitivity using a 1-D version of NEMO, *Geosci. Model Dev.*, *8*, 69–86, doi:10.5194/gmd-8-69-2015.

Reul, N., Y. Quilfen, B. Chapron, S. Fournier, V. Kudryavtsev, and R. Sabia (2014), Multisensor observations of the Amazon-Orinoco river plume interactions with hurricanes, *J. Geophys. Res. Oceans*, *119*, 8271–8295, doi:10.1002/2014JC010107.

Reverdin, G., E. Kestenare, C. Frankignoul, and T. Delcroix (2007), Surface salinity in the Atlantic Ocean (30° S-50° N), *Prog. Oceanogr.*, *73*, 311–340, doi:10.1016/j.pocean.2006.11.004.

Schade, L. R., and K. A. Emanuel (1999), The ocean's effect on the intensity of tropical cyclones: Results from a simple coupled atmosphere-ocean model, *J. Atmos. Sci.*, *56*(4), 642–651.

Umlauf, L., and H. Burchard (2003), A generic length-scale equation for geophysical turbulence models, *J. Mar. Res.*, *61* (31), 235–265.

Vincent, E. M., M. Lengaigne, G. Madec, J. Vialard, G. Samson, N. C. Jourdain, C. E. Menkes, and S. Jullien (2012a), Processes setting the characteristics of sea surface cooling induced by tropical cyclones, *J. Geophys. Res.*, *117*, C02020, doi:10.1029/2011JC007396.

Vincent, E. M., M. Lengaigne, J. Vialard, G. Madec, N. C. Jourdain, and S. Masson (2012b), Assessing the oceanic control on the amplitude of sea surface cooling induced by tropical cyclones, *J. Geophys. Res.*, *117*, C05023, doi:10.1029/2011JC007705.

Vincent, E. M., K. A. Emanuel, M. Lengaigne, J. Vialard, and G. Madec (2014), Influence of upper ocean stratification interannual variability on tropical cyclones, *J. Adv. Model. Earth Syst.*, *6*, 680–699, doi:10.1002/2014MS000327.

Vizy, E. K., and K. H. Cook (2010), Influence of the Amazon/Orinoco Plume on the summertime, Atlantic climate, *J. Geophys. Res.*, *115*, D21112, doi:10.1029/2010JD014049.

Wang, C., and D. B. Enfield (2001), The tropical Western Hemisphere warm pool. *Geophys. Res. Lett.*, *28*, 1635–1638.

Wentz, F. J., C. Gentemann, D. Smith, and D. Chelton (2000), Satellite measurements of sea-surface temperature through clouds, *Science*, *288*, 847–850.

White, R. H., and R. Toumi (2014), River flow and ocean temperatures: The Congo River, *J. Geophys. Res. Oceans*, *119*, 2501–2517, doi: 10.1002/2014JC009836.

Willoughby, H., R. Darling, and M. Rahn (2006), Parametric representation of the primary hurricane vortex. Part II: A new family of sectionally continuous profiles, *Mon. Weather Rev.*, *134*(4), 1102–1120.